

Tesi doctoral presentada per En/Na

Marc PERA TITUS

amb el títol

"Preparation, characterization and modeling of zeolite NaA membranes for the pervaporation dehydration of alcohol mixtures"

per a l'obtenció del títol de Doctor/a en

QUÍMICA

Barcelona, 29 de maig del 2006

Facultat de Química
Departament d'Enginyeria Química



UNIVERSITAT DE BARCELONA



This chapter focuses on the exposition and discussion of the results obtained concerning the preparation of both outer and inner-side tubular zeolite NaA membranes by the synthesis methods outlined in section III.1 (section IV.2). Moreover, some preliminary studies about the synthesis conditions of zeolite NaA powder and zeolite NaA layers onto glass supports have been also included (section IV.1). The effect of the main variables in the weight gain, N₂ permeation and He/N₂ selectivity after each synthesis cycle of the *as*-synthesized zeolite layers is shown in section IV.3. Furthermore, a more detailed characterization of some of the membranes by XRD and SEM is shown in section IV.4, which provides more complete information concerning the morphology and intergrowth of the zeolite layers. Finally, the pervaporation performance of the *as*-synthesized membranes towards the separation of ethanol/water mixtures is shown in section IV.5.

IV.1. PRELIMINARY STUDIES

IV.1.1. Synthesis of zeolite NaA crystals and layers

Prior to the synthesis of the zeolite NaA membranes, some preliminary studies were carried out to survey the optimal temperature and time conditions for hydrothermal synthesis of zeolite NaA crystals. Figure IV.1 shows the XRD patterns of the zeolite powder synthesized from gels 1, 2 and 4 (see Table III.3) in the temperature range 353-373 K for several synthesis times. As can be seen, pure zeolite NaA crystals could be obtained from gels 2 and 4 for synthesis times higher than 3 h. For the most concentrated gel (gel 1), pure zeolite NaA was synthesized just after 1 h. Gel 5 was found to be unsuitable for the preparation of zeolite NaA crystals, because the XRD patterns of the synthesized zeolite powder (not shown) revealed the presence of sodalite as main impurity. Moreover, zeolite NaA could be also hydrothermally synthesized onto the surface of glass flat supports previously seeded with zeolite NaA crystals (mean size, 7 μm) kept in a glass vessel at atmospheric pressure, as can be observed from the XRD patterns of the surface of the support shown in Figure IV.2. This result confirms the possibility to grow zeolite NaA layers onto the surface of a support. However, glass supports are not usually used for the preparation of zeolite NaA membranes, because they are highly hydrophobic (*Santamaria and Coronas, 1999*) and more hydrophilic supports such as α -alumina are usually preferred.

IV.1.2. Rheological characterization of the synthesis gels

Prior to the preparation of the membranes, the thixotropy of the synthesis gel 4, the most widely used in this work, was studied to determine its apparent viscosity. Figure IV.3 shows the evolution of the shear rate, $\dot{\gamma}$ [s^{-1}], and shear stress, τ [Pa], with time together with the

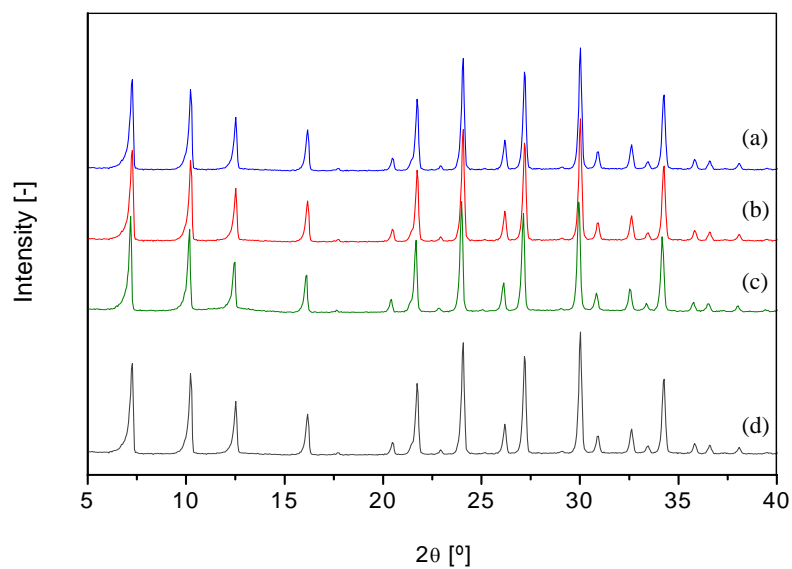


Figure IV.1: XRD patterns of pure zeolite NaA crystals synthesized in a discontinuous vessel with gel 2. Synthesis conditions: (a) T=373 K, time=7 h; (b) T=373 K, time=5 h; (c) T=373 K, time=3 h; and (d) T=353 K, time=5 h.

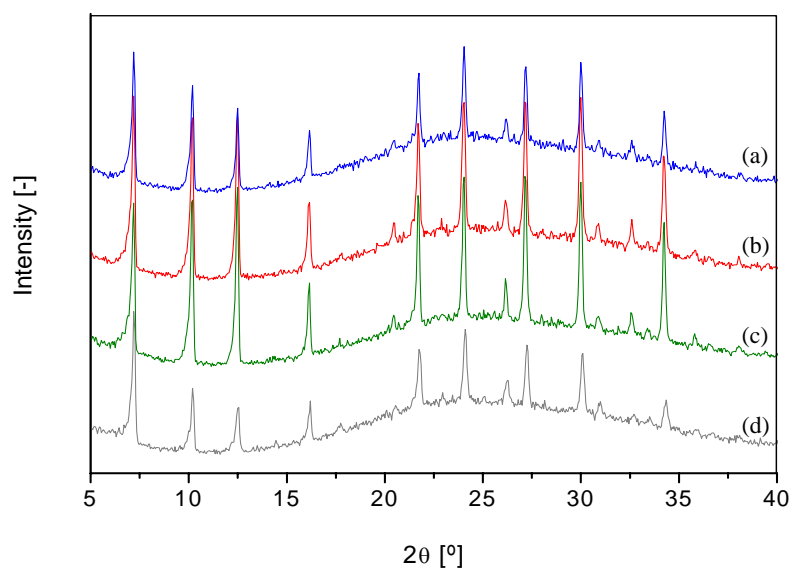


Figure IV.2: XRD patterns of zeolite NaA layers grown onto the surface of glass flat supports previously seeded with zeolite NaA crystals. Synthesis time of 5 h for all the layers. Other synthesis conditions: (a) gel 1, T=373 K; (b) gel 1, T=363 K; (c) gel 1, T=353 K; and (d) gel 2, T=363 K. All the peaks correspond to pure zeolite NaA. The wide central band is caused by the amorphous nature of glass.

dependence of the shear stress with the shear rate. The shear rate was chosen to evolve with time as depicted in Figure IV.3.a, that is, with a nul value during the first 15 min to allow the system to stabilize, followed by a linear rising trend during 15 min until a shear rate of 400 s^{-1} was reached. This value was stabilized for 15 min to determine the viscosity of the system, and further decreased during 15 min until 0. Figure IV.3b shows the evolution of the shear stress with time for the input shear rates in Figure IV.3a. Furthermore, the trend of the shear stress with the shear rate is plotted in Figure IV.3c, where 3 zones can be observed. Firstly, the shear stress tends to increase with the shear rate until the latter reaches a value of 400 s^{-1} , which is afterwards stabilized and finally decreases to 0 with a reduction of the shear rate. Figure IV.3d shows the stabilization of the shear stress at a constant shear rate of 400 s^{-1} , where it can be observed that the former tends to a steady-state value ca. 2.75 Pa. An aparent viscosity of $\mu_{\text{ap}} = \tau / \dot{\gamma} = 2.75 \text{ Pa} / 400 \text{ s}^{-1} = 6.9 \times 10^{-4} \text{ Pa s}$ has been determined from the

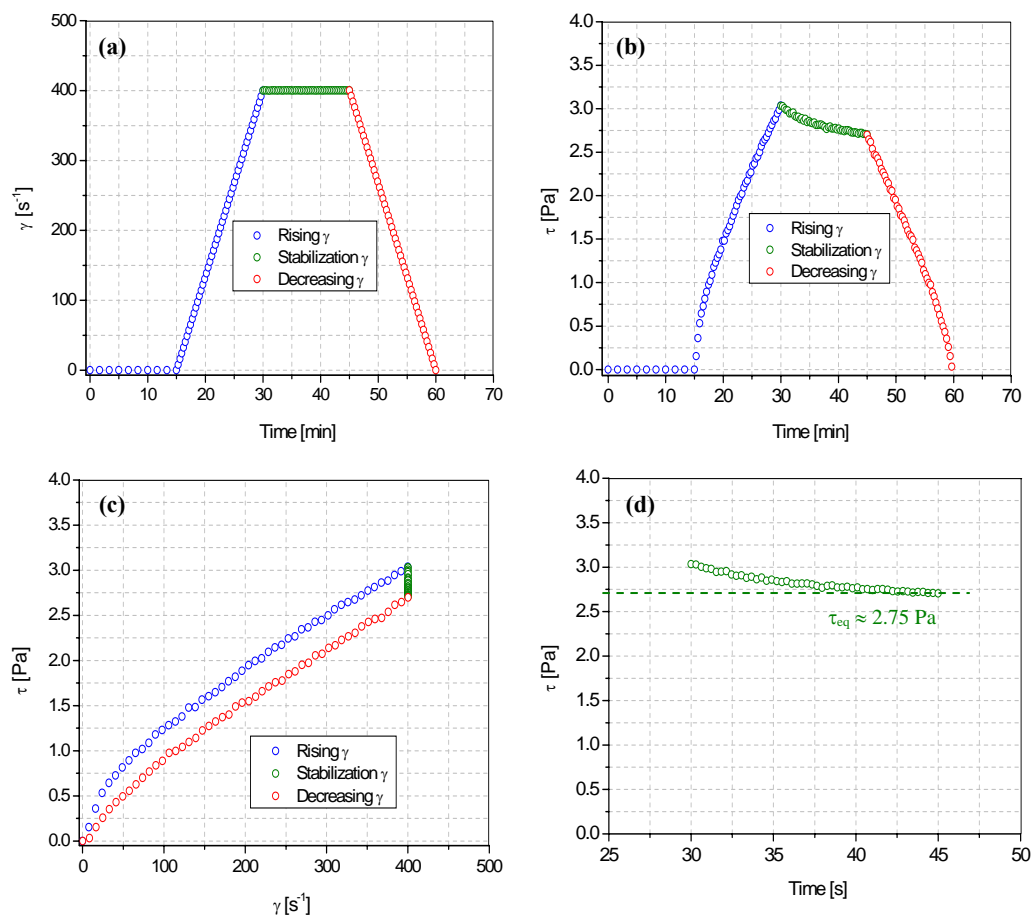


Figure IV.3: Tyxotropy of synthesis gel 4 at 293 K. (a) Evolution of $\dot{\gamma}$ with time; (b) Evolution of τ with time; (c) Evolution of the τ with the $\dot{\gamma}$; (d) Evolution of the τ with time at $\dot{\gamma} = 400 \text{ s}^{-1}$.

results exposed in Figure IV.3d for synthesis gel 4 at 293 K, which approaches the value reported for water at this temperature, $1.0 \times 10^{-3} \text{ kg m}^{-1} \text{ s}^{-1}$. In light of the low viscosity shown by synthesis gel 4 shows, it is expected to be able to circulate in a tube without much friction.

IV.2. CROSS-FLOW FILTRATION SEEDING: EFFECT OF THE OPERATING VARIABLES

A cross-flow seeding is presented in this work to allow a controlled seeding of zeolite NaA crystals from a suspension on the inner side surface of tubular supports. A steady-state amount of zeolite NaA crystals coating the support (i.e., seeding weight gain, SWG) can be attained by operating with a given suspension feed flow rate, zeolite NaA concentration, transmembrane pressure and pH. The permeability of the support decreases to a stable value, as the pores of the support become progressively blocked by the seeded zeolite NaA crystals (see Figure IV.4), and it is reduced from an initial value $\sim 40 \text{ mL min}^{-1} \text{ bar}^{-1}$ to $2 \text{ mL min}^{-1} \text{ bar}^{-1}$ within 2-3 h. Figure IV.4 also shows that, when working at low zeolite NaA concentrations in the suspension, all data can be roughly fitted by the same curve and thus the seeding pattern of the supports does not seem to depend on the zeolite NaA mean particle size or on the transmembrane pressure for the range used. This is a useful feature of the cross-flow filtration seeding procedure, as it shows that the process of covering the support surface with seeds is highly reproducible.

IV.2.1. Effect of feed flow rate

As can be seen in Figure IV.5, no effect of the feed flow rate in the SWG is observed at the surveyed feed flow rates for zeolite NaA concentrations in the suspension lower than 2500 mg L^{-1} . However, for the most concentrated solutions ($>5000 \text{ mg L}^{-1}$), a decrease of SWG with the feed flow rate is observed. In any case, as could be expected, SWG values increase with the concentration of the suspension.

IV.2.2. Effect of transmembrane pressure and particle size

The evolution of the SWG with the transmembrane mean pressure, ΔP_m , in the seeding process of α -alumina supports at a zeolite concentration of 20 ppm and at pH 8 is illustrated in Figure IV.6. As can be seen, the transmembrane pressure is progressively increased along the seeding process, typically from 1.0 to 3.0 bar, and the *transmembrane mean pressure* is

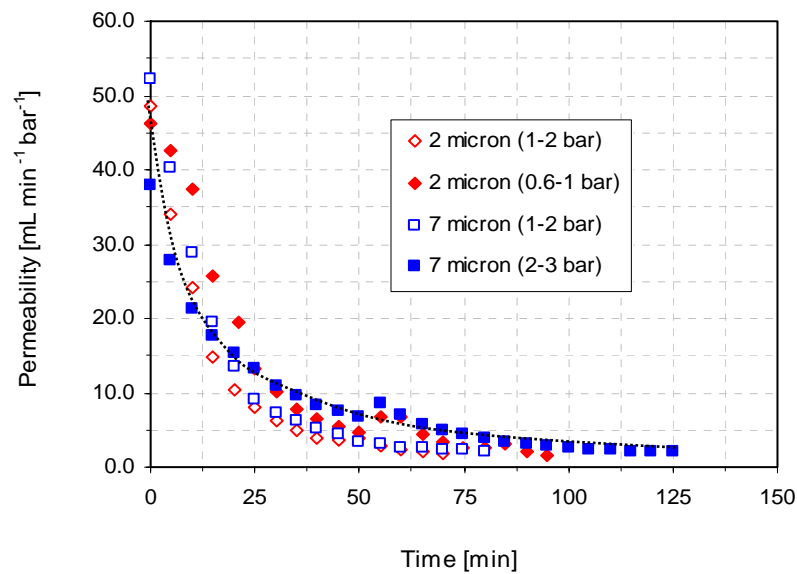


Figure IV.4: Evolution of water permeability during the cross-flow seeding process with 2 and 7 micron zeolite NaA particles at several transmembrane pressure ranges. Experimental conditions: pH=8, zeolite concentration=20 mg L⁻¹, feed flow rate=5.5 L min⁻¹. The dotted line refers to the trend observed.

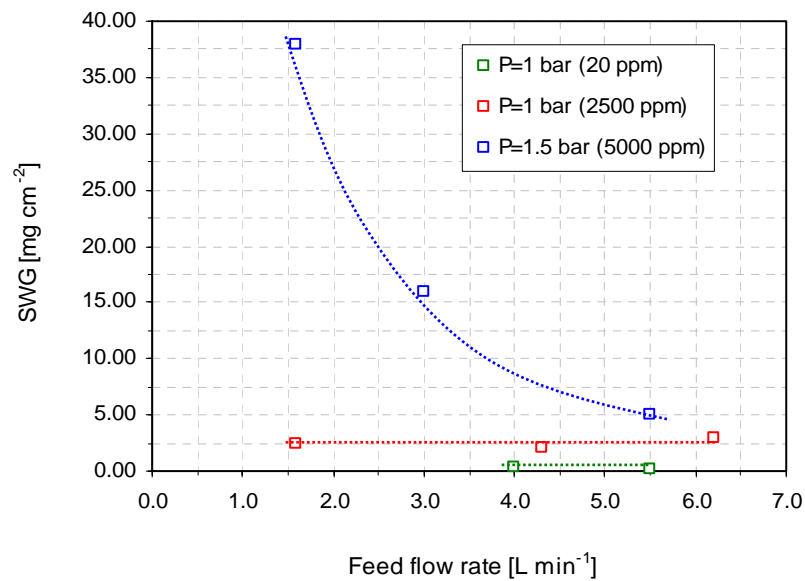


Figure IV.5: Evolution of steady-state seeding weight gain (SWG) with the feed flow in the cross-flow filtration seeding process for different transmembrane pressures (1 and 1.5 bar) and suspension zeolite concentrations (20, 2500, 5000 mg L⁻¹). Other experimental conditions: Mean particle size, 2 micron; pH=8. Dotted lines refer to the trends observed.

defined as a weighted transmembrane pressure of all its values along a seeding experiment. Despite the clear dispersion of the values obtained in Figure IV.6, an increasing trend of the SWG with ΔP_m is observed for 2 and 7 μm -zeolite mean particle sizes. This is an expected result, since a larger pressure drop increases the permeation flux across the membrane and more mechanical energy is supplied to the particles, which promotes their deposition onto the surface of the support.

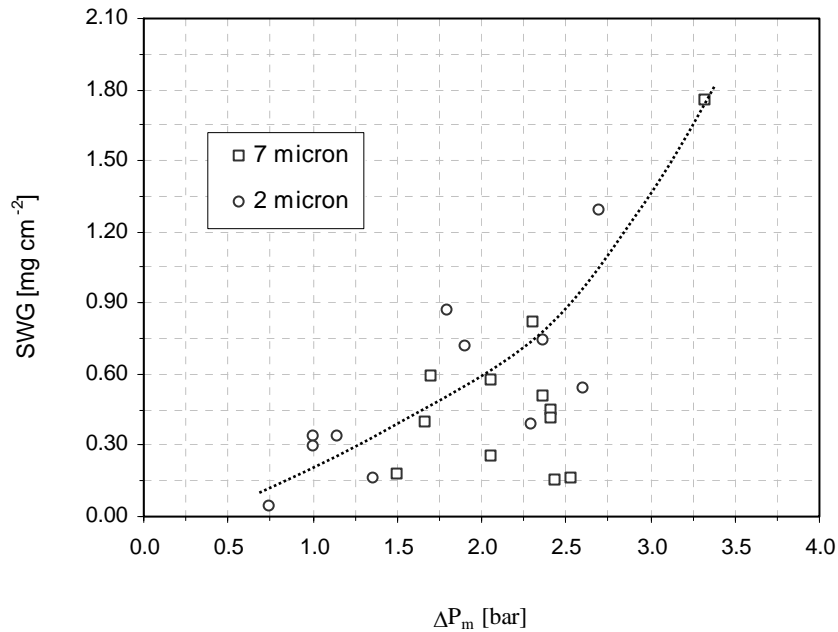


Figure IV.6: Evolution of steady-state seeding weight gain (SWG) with transmembrane mean pressure for the cross-flow filtration seeding process of α -alumina supports. Experimental conditions: Feed flow rate=5.5 L min⁻¹; mean particle size, 2 and 7 micron; pH=8. The dotted line refers to the trend observed.

IV.2.3. Effect of pH

Regarding the effect of the pH in the SWG (see Figure IV.7), a maximum in the SWG is observed around pH 8. This observation is consistent with the isoelectrical point (IEP) measurements carried out with zeolite NaA particles. The evolution of the ζ -potential of zeolite NaA suspensions (500 mg L⁻¹) with the pH (see Figure IV.8) reflects an IEP around 8, somewhat higher than the value of 7.2 reported by *Huang and Roads (1989)*. This value is slightly lower than the IEP of α - and γ -alumina (IEP~9.0) reported by *Yoops and Furstenuau (1964)* and *Huang and Roads (1989)*.

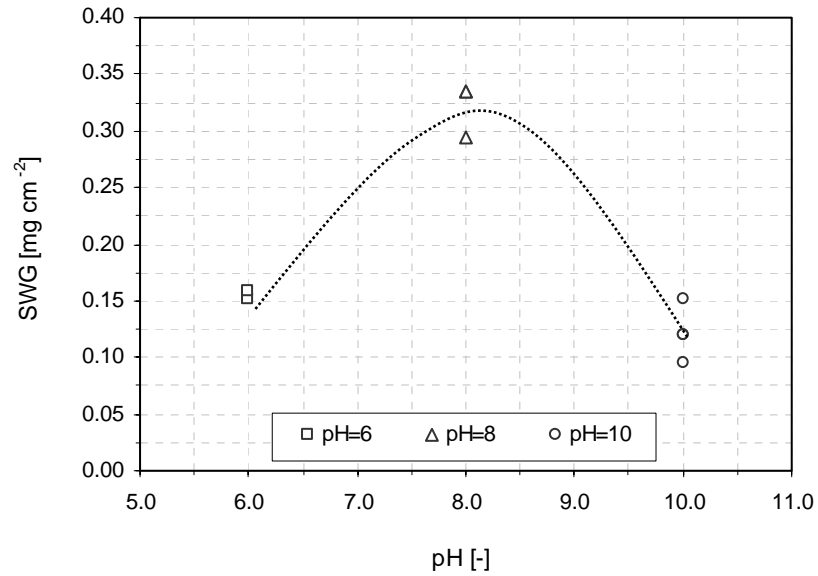


Figure IV.7: SWG as a function of pH in the cross-flow filtration seeding process for α -alumina supports with 1.0 bar transmembrane mean pressure difference. Experimental conditions: Mean particle size, 2 micron. Other conditions as in Figure IV.5. The dotted line refers to the trend observed.

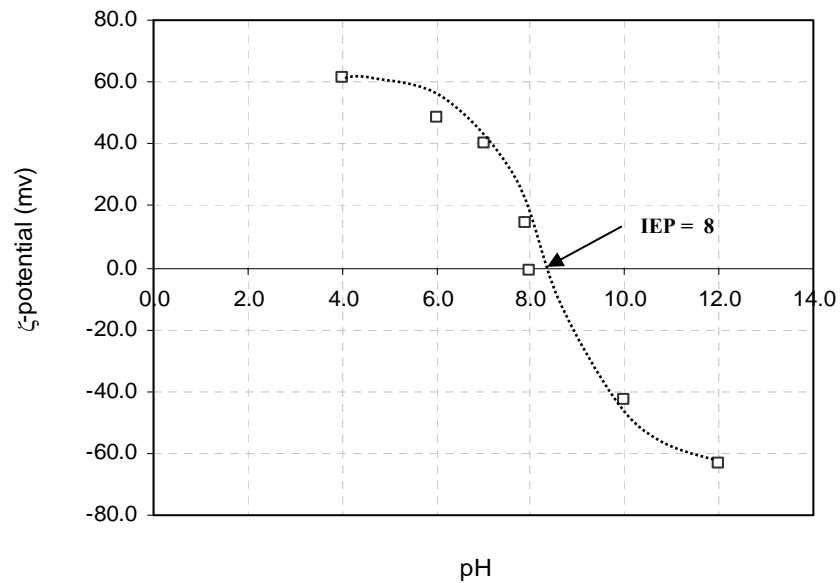


Figure IV.8: ζ -potential of zeolite NaA as a function of pH (mean particle size, 2 micron). The values indicated correspond to the mean of three consecutive replicates. The dotted line refers to the trend observed.

The trend observed in Figure IV.7 might be related to the charge on both the zeolite NaA particles and the α -alumina support. In this way, at pH values far from 8, both the zeolite NaA particles and the support would sustain charges of the same sign (positive at $\text{pH} < 8$ and negative at $\text{pH} > 9$). The resulting electrostatic repulsive forces could partially compensate the hydrodynamic effect of filtration in the deposition of particles onto the surface. However, as the pH approaches the IEP of zeolite NaA, attractive Van der Waals forces would be predominant and higher amounts of particles could be deposited onto the surface of the support and the trend of Figure IV.7 would be obtained (see Figure IV.9).

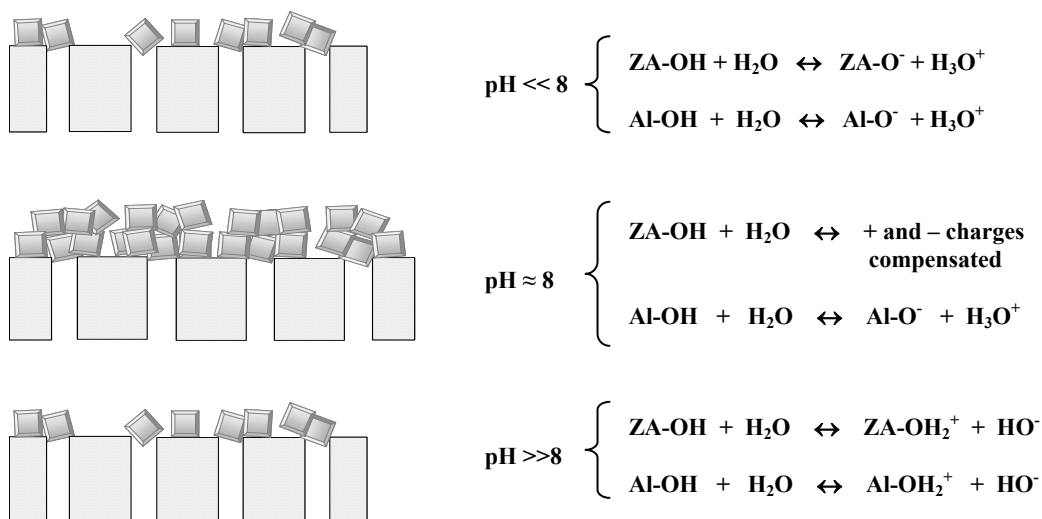


Figure IV.9: Effect of pH in the covering of the support with zeolite NaA particles in the cross-flow seeding process. As the pH approaches the IEP value of zeolite NaA, higher amounts of particles are deposited onto the surface of the support due to the increasing effect of attractive forces.

IV.3. PREPARATION OF OUTER- AND INNER-SIDE ZEOLITE NaA MEMBRANES

IV.3.1. Preparation of *outer-side* tubular zeolite NaA membranes in a discontinuous glass vessel with and without gel renewal

Table IV.1 shows the results concerning the outer-side tubular zeolite NaA membranes prepared in this work by the secondary growth method according to the protocols described in section III. The outer zeolite NaA layers were grown using gels 1 and 4 (see Table III.3) in one synthesis cycle with a previous seeding step using the rubbing technique. As can be seen in Table IV.1, the membranes prepared in the semi-continuous system show higher weight gains and lower N_2 permeances after 1 synthesis cycle than those prepared in a glass vessel

without gel renewal. In this way, the membranes synthesized with gel renewal show weight gains and N_2 permeances after synthesis in the range, respectively, 8-9 $mg\ cm^{-2}$ and 10^{-8} - 10^{-9} $mol\ m^{-2}\ s^{-1}\ Pa^{-1}$, while those synthesized in a static discontinuous vessel show values in the range, respectively, 4-5 $mg\ cm^{-2}$ and around 10^{-7} $mol\ m^{-2}\ s^{-1}\ Pa^{-1}$, respectively. Therefore, refreshment of the synthesis gel tends to improve the quality of the *as*-synthesized zeolite NaA layers by increasing the amount of zeolite NaA material covering the support and by reducing the number of meso- and macroporous defects in the zeolite layers. However, no clear trends for the weight gain and N_2 permeance after synthesis with the renewal rate can be observed for the membranes synthesized in the semi-continuous system. Furthermore, it should be noted that, regarding the results exposed in Table IV.1, the preparation of outer-side zeolite NaA membranes in the semi-continuous system seems to be fairly reproducible in terms of weight gain and N_2 permeance.

Table IV.1: Seeding and synthesis tested conditions for the outer-side tubular zeolite NaA membranes prepared in one synthesis cycle (T=368-373 K)

<i>Membrane</i>	<i>Gel</i>	<i>Time [h]</i>	<i>Renewal rate [min^{-1}]</i>	<i>SWG [$mg\ cm^{-2}$]</i>	<i>Weight gain [$mg\ cm^{-2}$]</i>	<i>N_2 permeance [$mol\ m^{-2}\ s^{-1}\ Pa^{-1}$]</i>
ZA-OUT-01	1	3	0 ($1/\infty$)	0.10	4.35	1.17×10^{-7}
ZA-OUT-02*	1	3	0 ($1/\infty$)	0.10	6.20	4.43×10^{-7}
ZA-OUT-SC -01	4	5	1/38	0.48	6.37	1.98×10^{-9}
ZA-OUT-SC -02	4	5	1/25	0.45	7.98	1.31×10^{-9}
ZA-OUT-SC -03	4	5	1/20	0.51	8.08	7.82×10^{-10}
ZA-OUT-SC -04	4	5	1/16	0.46	9.03	1.54×10^{-9}
ZA-OUT-SC -05	4	5	1/13	0.73	8.11	1.18×10^{-8}

* 2 synthesis cycles

IV.3.2. Preparation of inner-side tubular zeolite NaA membranes in a discontinuous glass vessel with and without the presence of a centrifugal field

The synthesis conditions for the most relevant inner-side tubular membranes prepared either with or without the presence of a centrifugal field are summarized in Table IV.2. In Table IV.2, data concerning weight gain, N_2 permeation and He/ N_2 ideal selectivity after 2-4 synthesis cycles are also indicated. This section focuses firstly on the evaluation of the reproducibility of the given recipe for the synthesis of these membranes. Afterwards, the evaluation of the influence of a centrifugal field, as well as the effect of the gel concentration and the seeding weight gain (SWG), in the preparation of the membranes constitutes the subject of study.

Table IV.2: Seeding and synthesis tested conditions for the inner-side tubular zeolite NaA membranes prepared either with or without the presence of a centrifugal field (T=373 K; synthesis time=3 h)

<i>Membrane</i> [*]	<i>Gel</i>	<i>No. of cycles</i>	<i>SWG [mg cm⁻²]</i>	<i>Weight gain [mg cm⁻²]</i>	<i>N₂ permeance [mol m⁻² s⁻¹ Pa⁻¹]</i>	<i>He/N₂ ideal selectivity [-]</i>
ZA-INN-CF -01	1	4	0.40	11.4	4.35 × 10 ⁻⁷	2.30
ZA-INN-CF -02	1	3	0.20	9.1	2.31 × 10 ⁻⁶	2.06
ZA-INN-CF -03	2	3	0.45	4.7	1.26 × 10 ⁻⁷	2.37
ZA-INN-CF -04	2	3	0.41	5.7	1.83 × 10 ⁻⁷	2.28
ZA-INN-CF -05	2	3	0.15	2.4	5.40 × 10 ⁻⁸	1.89
ZA-INN-CF -06	2	4	1.75	7.4	4.77 × 10 ⁻⁷	2.32
ZA-INN-CF -07	4	3	0.15	1.9	1.22 × 10 ⁻⁶	1.74
ZA-INN-CF -08	5	2	0.08	7.6	4.60 × 10 ⁻⁸	2.59
ZA-INN-CF -09	1	3	0.05	13.4	8.70 × 10 ⁻⁷	1.77
ZA-INN-CF -10	1	3	1.60	13.7	3.14 × 10 ⁻⁶	1.96
ZA-INN -01	1	3	0.15	1.34	7.60 × 10 ⁻⁶	1.35

^{*} For membranes prepared under a centrifugal field, the rotation speed was kept at 100 r.p.m.

IV.3.2.1. Effect of the presence of a centrifugal field

Figures IV.10-IV.12 shows the effect of rotation of the support at 100 r.p.m in the weight gain, N₂ permeance and He/N₂ ideal selectivity of two as-synthesized zeolite NaA membranes. As can be seen in Figure IV.11, membrane ZA-INN-CF-05 prepared under a centrifugal field shows a sharper decrease of the N₂ permeance (especially after the 1st synthesis cycle) compared to membrane ZA-INN-1 prepared under the same conditions but statically (the N₂ permeance of the seeded supports is ~10⁻⁵ mol m⁻² s⁻¹ Pa⁻¹). The increased reduction in the N₂ permeance due to a centrifugal field is consistent with the hypothesis put forward in section III.1.5 that a centrifugal field might promote the segregation of the gel inside the tubular support and thus an improvement of its refreshment due to the action of a density gradient along the rotating support. However, according to Figure IV.10, the rotation of the support does not seem to exert much influence on the weight gain (it increases regularly after each synthesis cycle to a value around 2.5 mg cm⁻² after the 3rd cycle). Furthermore, according to Figure IV.12, a centrifugal field also seems to improve slightly the He/N₂ ideal selectivity and thus the quality of the membranes prepared, which would be related to the growth of a layer with a lower amount of defects. The He/N₂ ideal selectivity values do not change much after each synthesis cycle, which could imply that the configuration of the zeolite layer does not practically change after the first synthesis cycle. In fact, the first synthesis cycle seems to be the most relevant in the growth of zeolite NaA layers.

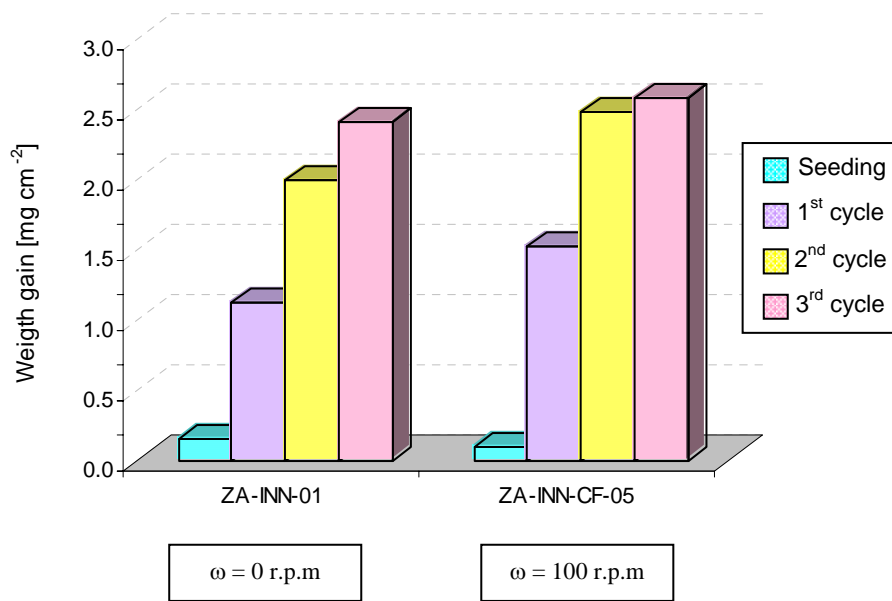


Figure IV.10: Evolution of weight gain with the number of synthesis cycles either with or without the presence of a centrifugal field in the preparation of inner-side tubular zeolite NaA membranes. Synthesis conditions: T=373 K; synthesis time=3 h; synthesis with gel 1; SWG=0.10-0.15 mg cm⁻²).

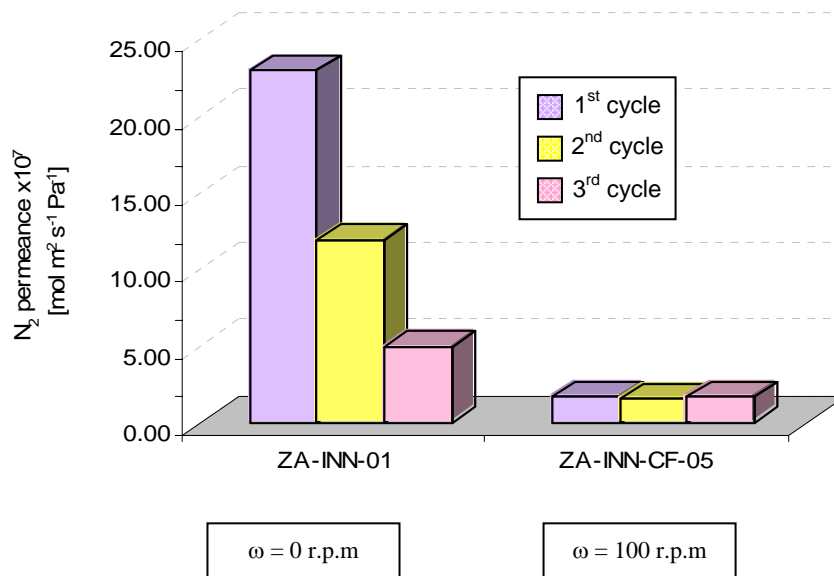


Figure IV.11: Evolution of the N₂ permeance with the number of synthesis cycles either with or without the presence of a centrifugal field in the preparation of inner-side tubular zeolite NaA membranes. Synthesis conditions as in Figure IV.10.

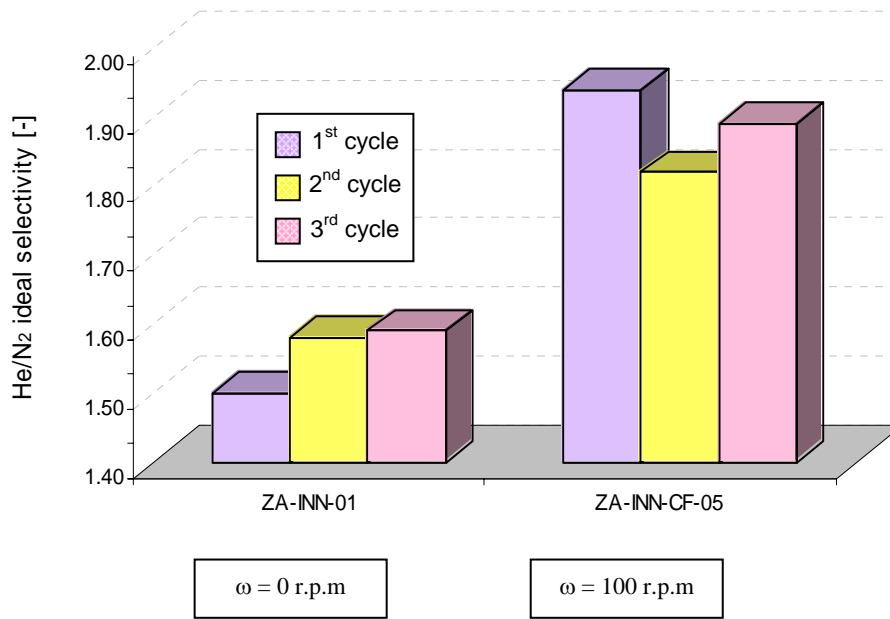


Figure IV.12: Evolution of the He/N₂ ideal selectivity with the number of synthesis cycles either with or without the presence of a centrifugal field in the preparation of inner-side tubular zeolite NaA membranes. Synthesis conditions as in Figure IV.10.

IV.3.2.2. Effect of the concentration of the gel

The effect of the concentration of the gel in the weight gain, N₂ permeance and He/N₂ ideal selectivity values of the *as*-synthesized membranes is shown in Figures. IV.13-IV.15. As can be seen in Figure IV.13, the weight gain after each synthesis cycle increases with the concentration of the synthesis gel, which might be related to a faster supply of the nutrients to the growing zeolite layer.

On the other hand, according to Figure IV.14, in the syntheses carried out with the most concentrated gels (gels 1 and 2) under a centrifugal field, the first cycle typically gives rise to a drop of two orders of magnitude in the N₂ permeance to that of the fresh support, thus confirming the results pointed out in section IV.3.2.1. However, for gel 3, although the N₂ permeance decreases progressively with the number of synthesis cycles, the N₂ permeance shows higher values. It should be highlighted that these trends aforementioned are consistent with the He/N₂ selectivities (see Figure IV.15), whose values are close to the ideal Knudsen selectivity (2.64) for the membranes prepared with gels 1, 2 and 5. Nevertheless, lower He/N₂ selectivities are obtained for the membranes synthesized with gel 3, thus suggesting the presence of a higher concentration of defects due to lower layer intergrowth.

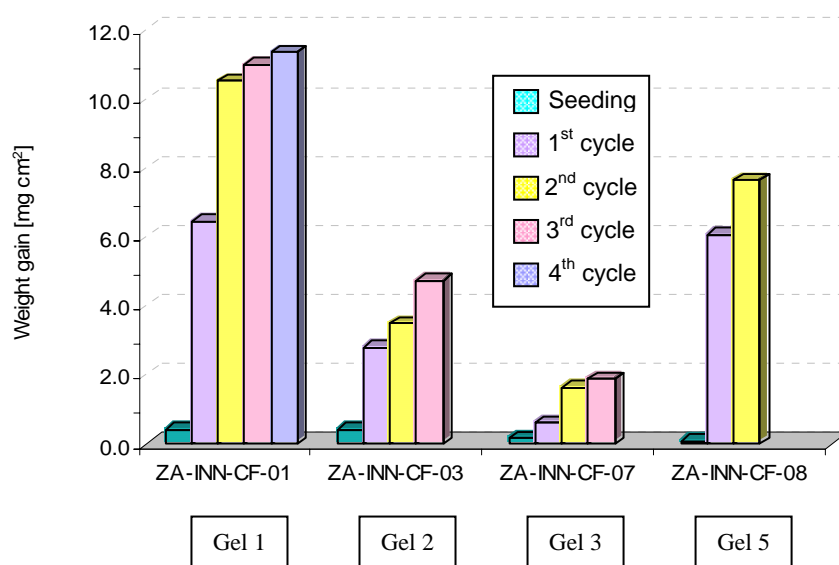


Figure IV.13: Evolution of the weight gain after synthesis with the gel concentration for inner-side tubular zeolite NaA membranes prepared under a centrifugal field. Synthesis conditions: T=373 K; synthesis time=3 h; $\omega=100$ r.p.m; SWG=0.08-0.40 mg cm⁻².

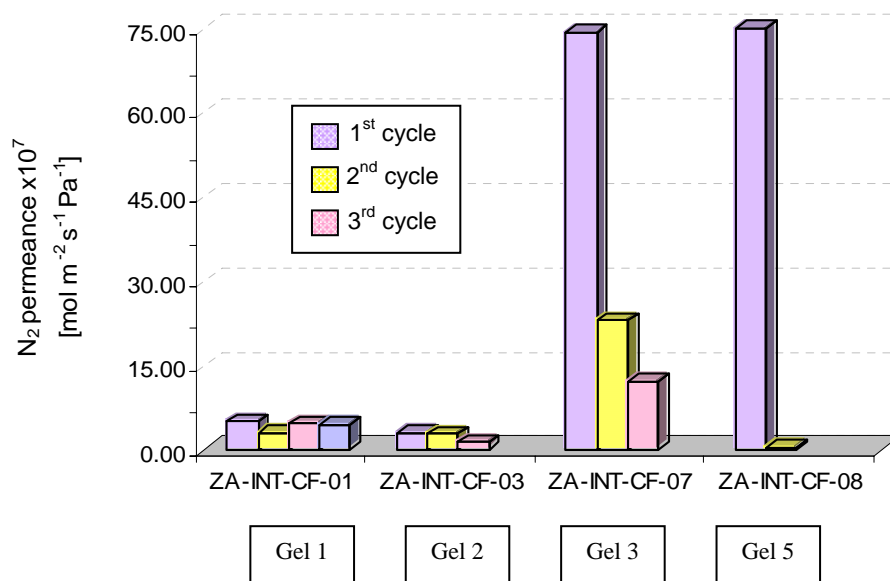


Figure IV.14: Evolution of the N₂ permeance with the gel concentration for inner-side tubular zeolite NaA membranes prepared under a centrifugal field. Synthesis conditions as in Figure IV.13.

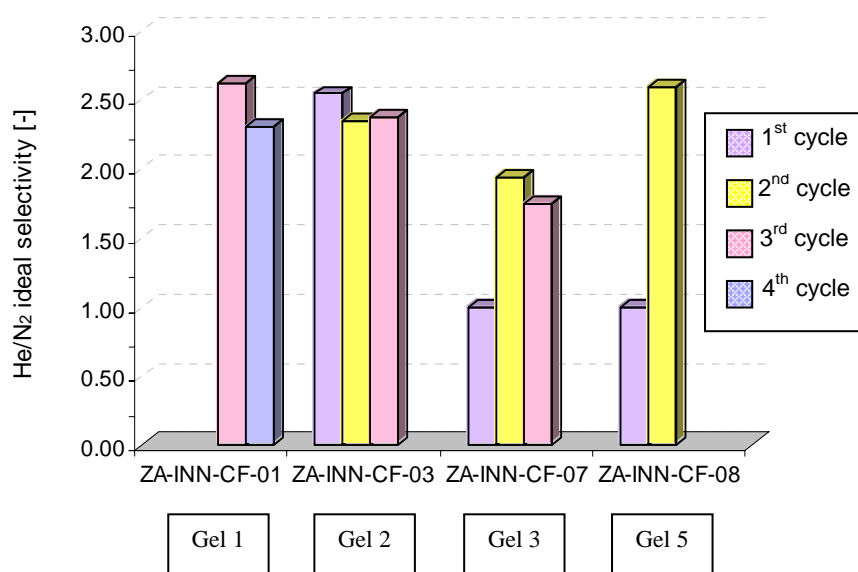


Figure IV.15: Evolution of the He/N₂ ideal selectivity with the gel concentration for inner-side tubular zeolite NaA membranes prepared under a centrifugal field. Synthesis conditions as in Figure IV.13.

IV.3.2.3. Effect of the seeding weight gain (SWG)

The SWG seems to play an important role in the final properties of the *as*-synthesized membranes prepared (see Figures IV.16-IV.18). As could be expected, the weight gain of the *as*-synthesized membranes increases with the SWG after each synthesis cycle (see Figure IV.16). Thus, for the unseeded membrane ZA-INN-01 (*in situ* hydrothermal synthesis), the weight gain after 3 synthesis cycles was approximately 1.3 mg cm⁻². This value increased to almost 4.5 mg cm⁻² for the membrane ZA-INN-CF-03 with a SWG value of 0.40 mg cm⁻², and to 7.3 mg cm⁻² for membrane ZA-INN-CF-06 with a SWG value of 1.75 mg cm⁻².

Moreover, according to Figures IV.17 and IV.18, the N₂ permeance and the He/N₂ ideal selectivity of the *as*-synthesized membranes seem to be also dependent on their SWG values. The membranes prepared in a SWG range of 0.15-0.41 mg cm⁻² with gels 1 and 2 show the highest reduction of the N₂ permeance, ca. two orders of magnitude, while those prepared without a previous seeding step or with high SWG values show lower reductions. The observed trends agree fairly well with the He/N₂ ideal selectivity values, lying around 2.4-2.5 after the 1st synthesis cycle for the membranes prepared in the SWG range of 0.15-0.41 mg cm⁻², while those prepared with lower SWG values show lower He/N₂ selectivity values.

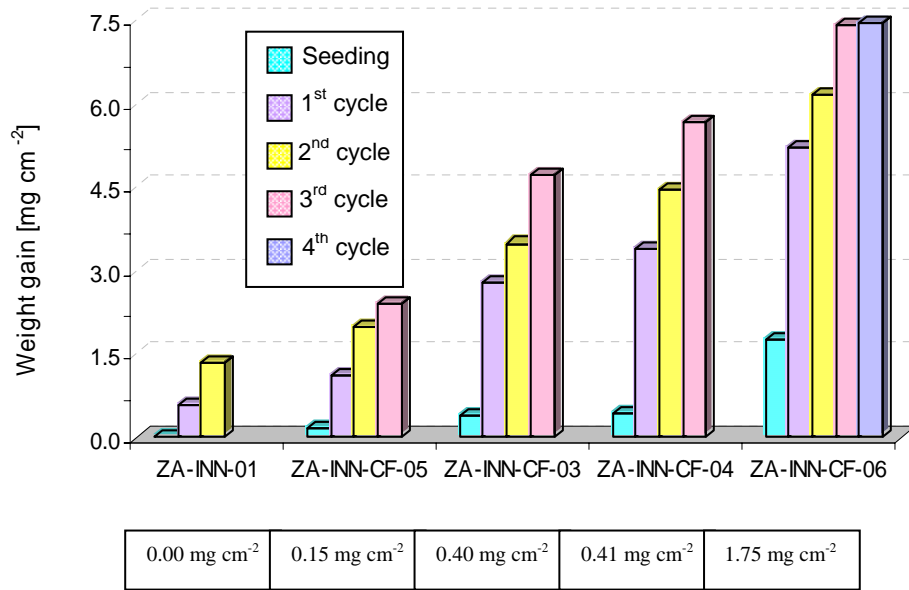


Figure IV.16: Evolution of the weight gain after synthesis with the SWG for inner-side tubular membranes prepared under a centrifugal field. Synthesis conditions: T=373 K; synthesis time=3 h; synthesis with gel 2 for all the membranes except for membrane ZA-INN-CF-05, where gel 1 was used; $\omega=100$ r.p.m; SWG=0.08-0.40 mg cm⁻².

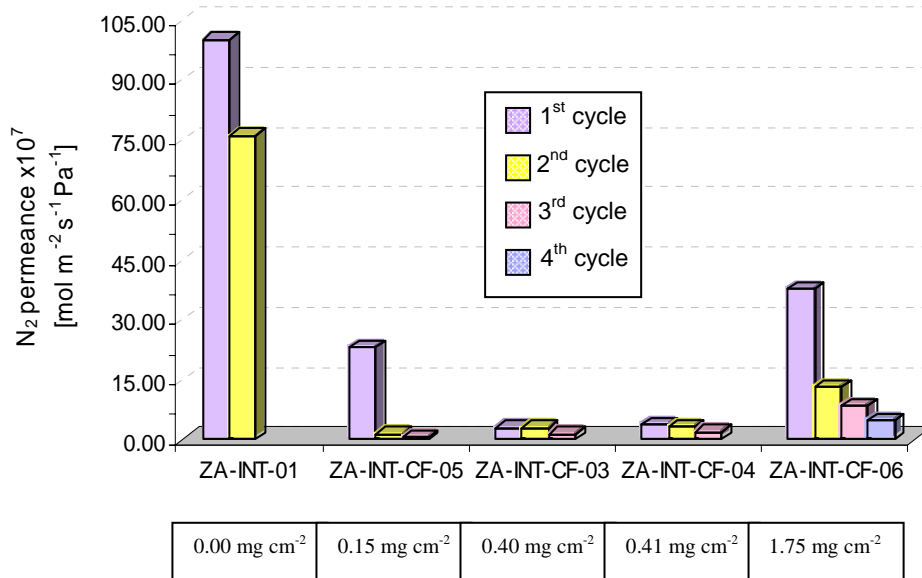


Figure IV.17: Evolution of the N₂ permeance with the SWG for inner-side tubular membranes prepared under a centrifugal field. Synthesis conditions as in Figure IV.16.

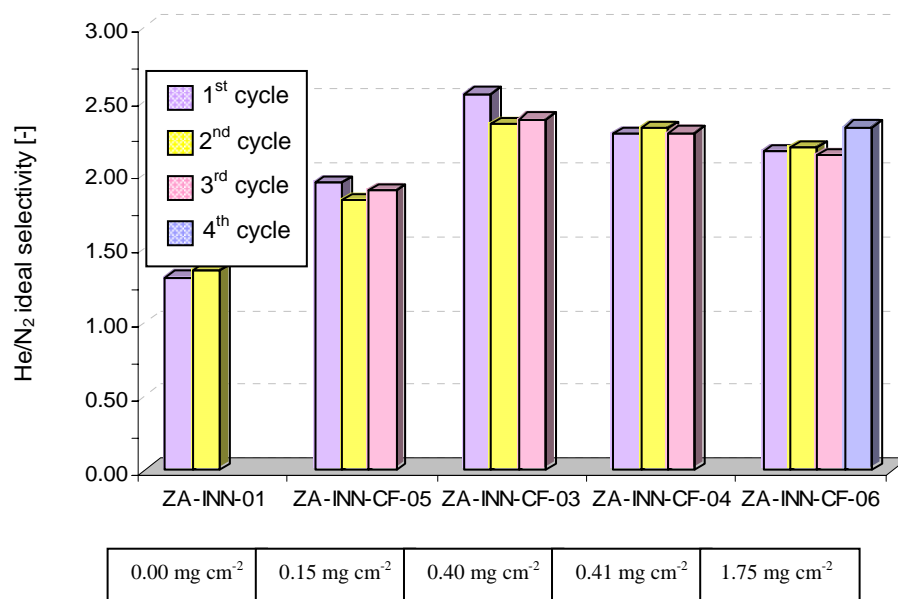


Figure IV.18: Evolution of the He/N₂ ideal selectivity with SWG for inner-side tubular membranes prepared under a centrifugal field. Synthesis conditions as in Figure IV.16.

Furthermore, according to Figures IV.16-IV.18, membranes ZA-INN-CF-03 and ZA-INN-CF-04 prepared under identical cross-flow seeding conditions (SWG ≈ 0.40 mg cm⁻²) and hydrothermal synthesis conditions (gel 2, T=373 K), show very close weight gain values ~ 5 mg cm⁻² after 3 synthesis cycles. Moreover, regarding the N₂ permeance and He/N₂ selectivity data, both membranes show, respectively, values of the same order, which indicates that, in both cases, the synthesized zeolite NaA layers have a similar amount of defects and flux pattern (for both membranes, the N₂ permeances is $\sim 10^{-7}$ mol m⁻² s⁻¹ Pa⁻¹, while the He/N₂ selectivities are ~ 2). Since the He/N₂ ideal selectivity values are lower than the ideal Knudsen selectivity (2.64), it can be concluded that a number of meso- and macroporous defects exists in the layer. However, the number of large pores is low according to the results obtained from Knudsen-Laminar tests, which revealed Knudsen ratios of 80 and 95%, respectively, for membranes ZA-INN-CF-03 and ZA-INN-CF-04.

IV.3.3. Preparation of inner-side tubular zeolite NaA membranes in a semi-continuous system

The semi-continuous system employed for the synthesis of outer-side tubular zeolite NaA membranes was also used for the synthesis of inner-side tubular zeolite NaA membranes.

Table IV.3 summarizes the synthesis conditions and results concerning the weight gain and N₂ permeance of the membranes prepared using different arrangements inside the autoclave (see Figure III.8), renewal rates, seeding method, SWG values and number of synthesis cycles (1-2). All the inner-side zeolite NaA layers were grown using gel 4 in the autoclave depicted in Figure III.8. The zeolite layers were prepared by setting the supports on the bottom of the autoclave in an intermediate vertical position with the help of a base, or either by attaching them to the gel inlet or outlet tubes of the autoclave in the synthesis process, as was exposed in section III.1.6.

IV.3.3.1. Effect of the position of the membrane in the autoclave

The effect of the position of the membrane inside the autoclave (i.e., at the bottom in a vertical position with the help of a base or either attached to the gel inlet or outlet tubes) was first evaluated in terms of weight gain and N₂ permeance (see Figures IV.19 and IV.20). As can be seen, for the membranes prepared with SWG values in the range 0.16-0.29 mg cm⁻² and a renewal rate of 1/16 min⁻¹ in 1 synthesis cycle, those attached to the gel inlet tube show slightly higher weight gain values and lower N₂ permeances after synthesis than those attached to the gel outlet tube. Furthermore, although the membranes placed at the bottom of the autoclave show weight gain values of the same order of magnitude as that of the membranes attached to the gel inlet tube, their N₂ permeances are much higher, which might involve the presence of a higher number of large defects in the zeolite layers.

According to these results, attaching the membranes to the gel inlet tube of the autoclave (Figure III.8b) appears to be the most appropriate arrangement according to the results listed in Table IV.3. Thus, when comparing the membranes in the first half of Table IV.3 (those with renewal rates in the 1/13-1/25 min⁻¹ range) it can be seen that the membranes prepared with arrangement III.8b present the lowest N₂ permeance values. For instance, while membranes ZA-INN-SC-13 and ZA-INN-SC-14 prepared in such a configuration show N₂ permeance values of 4.86×10^{-8} and 6.79×10^{-8} mol m⁻² s⁻¹ Pa⁻¹, respectively, the membranes prepared under the same synthesis conditions but using arrangements III.8a (ZA-INN-SC-02 and ZA-INN-SC-03) and III.8c (ZA-INN-SC-07), show N₂ permeance values that are of one order of magnitude higher.

The effect of the feed/membrane arrangements of Figure III.8 can be explained by taking into account the fact that, in arrangement III.8b (membrane coupled to gel inlet) a complete renovation of the gel inside the lumen of the tubes is achieved at every gel renewal and therefore synthesis takes place with gel concentrations that are closer to those of the fresh feed. This is in contrast with the situation in configuration III.8a, where gel renewal inside the tube is achieved only through a diffusion process. On the other hand, arrangement III.8c seems

Table IV.3: Synthesis conditions, weight gain after synthesis and nitrogen permeance for the membranes prepared in the semi-continuous system (synthesis carried out at 368 K, 5 h per cycle).

Membrane	Seeding method ¹	Arrangement (see Figure III.8) ²	Renewal rate [min ⁻¹]	No. of synthesis Cycles	SWG [mg cm ⁻²]	Weight gain [mg cm ⁻²]	N ₂ permeance [mol m ⁻² s ⁻¹ Pa ⁻¹]
ZA-1NN-SC-01	Filtration	a	1/25	1	6.25	6.71	>1.00 × 10 ⁻⁵
ZA-1NN-SC-02	Filtration	a	1/16	1	0.16	4.97	2.91 × 10 ⁻⁷
ZA-1NN-SC-03	Filtration	a	1/16	1	0.54	6.97	2.36 × 10 ⁻⁷
ZA-1NN-SC-04	Filtration	a	1/13	1	0.39	2.94	3.88 × 10 ⁻⁸
				2		4.59	1.52 × 10 ⁻⁷
ZA-1NN-SC-05	Filtration	c	1/25	1	0.33	5.39	>1.00 × 10 ⁻⁵
ZA-1NN-SC-06	Filtration	c	1/20	1	1.50	5.01	6.53 × 10 ⁻⁸
ZA-1NN-SC-07	Filtration	c	1/16	1	0.74	4.61	9.81 × 10 ⁻⁷
ZA-1NN-SC-08	Filtration	c	1/16	1	0.25	2.67	2.79 × 10 ⁻⁷
				2		5.93	2.45 × 10 ⁻⁷
ZA-1NN-SC-09	Filtration	c	1/16	1	0.21	2.57	7.48 × 10 ⁻⁸
ZA-1NN-SC-12	Filtration	b	1/16	1	0.87	5.37	2.70 × 10 ⁻⁶
ZA-1NN-SC-13	Filtration	b	1/16	1	0.29	3.95	4.86 × 10 ⁻⁸
ZA-1NN-SC-14	Filtration	b	1/16	1	0.18	4.78	6.79 × 10 ⁻⁸
ZA-1NN-SC-16	Filtration	b	1/7	1	0.82	8.09	1.01 × 10 ⁻⁶
ZA-1NN-SC-17	Filtration	b	1/7	1	0.51	3.97	1.47 × 10 ⁻⁶
ZA-1NN-SC-18	Filtration	b	1/7	1	0.15	10.14	3.39 × 10 ⁻⁹
				2		19.16	1.58 × 10 ⁻⁸
ZA-1NN-SC-19	Filtration	b	1/7	1	0.15	10.89	5.96 × 10 ⁻⁹
				2		19.57	3.65 × 10 ⁻⁹
ZA-1NN-SC-20	Filtration	b	1/7	1	0.10	7.92	5.58 × 10 ⁻⁸
				2		15.39	4.84 × 10 ⁻⁸

Table IV.3 (to be continued)

Membrane	Seeding method ¹	Arrangement (see Figure III.8) ²	Renewal rate [min ⁻¹]	No. of synthesis Cycles	SWG [mg cm ⁻²]	Weight gain [mg cm ⁻²]	N ₂ permeance [mol m ⁻² s ⁻¹ Pa ⁻¹]
ZA-INN-SC-21	Filtration	b	1/4	1	0.57	5.91	8.39 x 10 ⁻⁷
ZA-INN-SC-22	Filtration	b	1/4	1	0.12	14.86	1.74 x 10 ⁻⁸
				2		25.48	<1.00 x 10 ⁻⁹
ZA-INN-SC-23	Filtration	b	1/4	1	0.12	9.02	1.46 x 10 ⁻⁸
				2		16.01	3.57 x 10 ⁻⁹
ZA-INN-SC-24	Brush	b	1/7	1	0.19	15.98	1.36 x 10 ⁻⁸
ZA-INN-SC-25	Brush	b	1/7	1	0.16	27.18	1.65 x 10 ⁻⁸
ZA-INN-SC-26	Brush	b	1/7	1	0.12	4.87	8.64 x 10 ⁻⁹
				2		-	<1.00 x 10 ⁻⁹
ZA-INN-SC-27	Brush	b	1/7	1	0.12	10.12	8.06 x 10 ⁻⁹
				2		17.08	2.06 x 10 ⁻⁸
ZA-INN-SC-28	Brush	b	1/4	1	0.13	10.72	4.82 x 10 ⁻⁸
				2		17.60	<1.00 x 10 ⁻⁹
ZA-INN-SC-29	Brush	b	1/4	1	0.13	19.83	1.99 x 10 ⁻⁸
				2		41.02	2.88 x 10 ⁻⁹
ZA-INN-02	Brush	b	-	1	0.15	1.34	7.60 x 10 ⁻⁶

¹ For cross-flow filtration seeding the following conditions were used: feed flow rate 5.5 L min⁻¹; seed concentration 20 mg L⁻¹; mean seed size 2 μm; pH range 6-10; transmembrane pressure 1-3 bar

² Attachments: (a) Membrane set in an intermediate vertical position
 (b) Membrane attached to the gel inlet tube
 (c) Membrane attached to the gel outlet tube

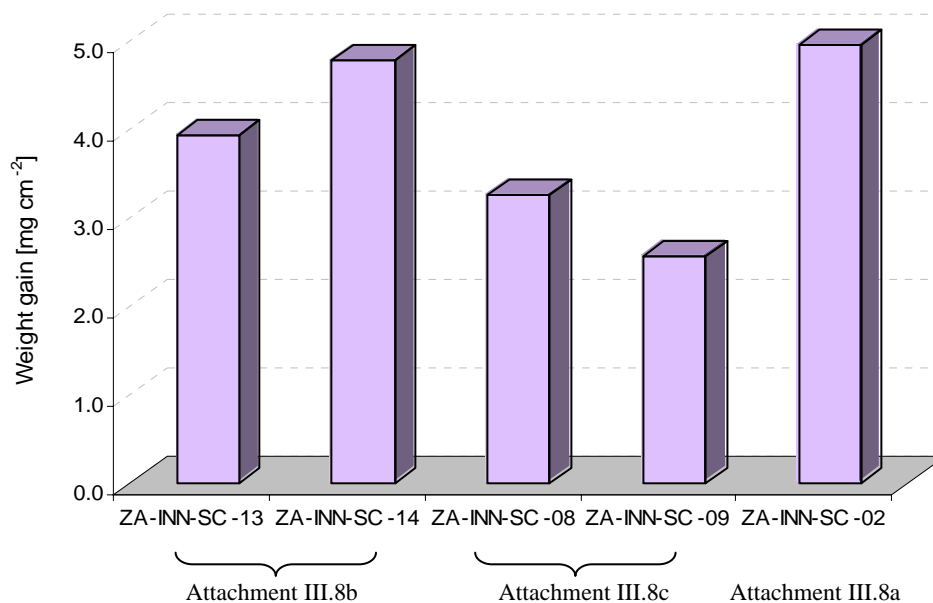


Figure IV.19: Evolution of the weight gain after the 1st synthesis cycle for membranes prepared in the semi-continuous system with arrangements III.8a-c in the autoclave. Synthesis conditions: T=368 K; synthesis time=5 h; synthesis with gel 4; renewal rate=1/16 min⁻¹; SWG≈0.16-0.29 mg cm⁻².

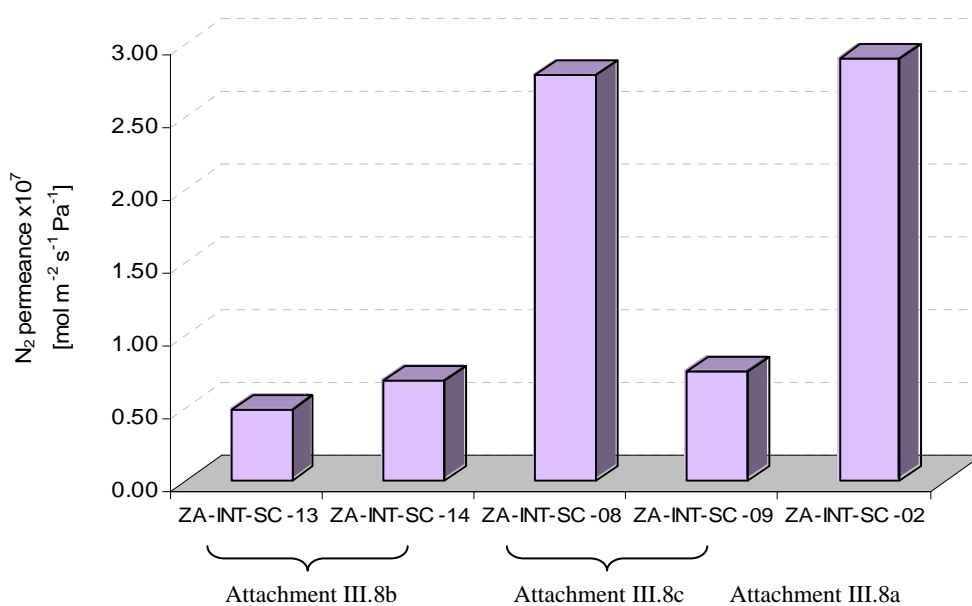


Figure IV.20: Evolution of the N₂ permeance after the 1st synthesis cycle for the membranes prepared in the semi-continuous system with arrangements III.8a-c in the autoclave. Synthesis conditions as in Figure IV.19.

more favorable, since a positive flow along the support tube also forces renewal of the gel inside the support. However, the gel introduced by this net flow into the support comes from the bulk of the autoclave, and therefore reactant concentration has already undergone significant depletion. In view of these results, it was decided to use attachment III.8b to study the effect of higher renewal rates, as shown in the second half of Table IV.3.

Furthermore, as can be derived from Table IV.3, membranes ZA-INN-SC-18, ZA-INN-SC-19 and ZA-INN-SC-20 prepared with a SWG value in the range 0.10-0.15 mg cm⁻² and with a renewal rate 1/7 min⁻¹ with gel 4 show close weight gain values after the first and second synthesis cycles in the range 8-11 mg cm⁻² after the 1st cycle and 15-20 mg cm⁻² after the 2nd one. Moreover, the N₂ permeances determined for these membranes lie in the range 0.36-4.80 × 10⁻⁸ mol m⁻² s⁻¹ Pa⁻¹ after two synthesis cycles, which are over three orders of magnitude lower than the value corresponding to the support (~10⁻⁵ mol m⁻² s⁻¹ Pa⁻¹). This result suggests that the zeolite NaA layers prepared have in both cases the same order of defects and the same flux pattern.

IV.3.3.2. Effect of the gel renewal rate

The effect of the renewal rate for some membranes prepared under otherwise comparable synthesis conditions is depicted in Figure IV.21. As can be seen, an increase in the weight gain and a reduction of the N₂ permeance after synthesis occurs for higher renewal rates, indicating that layer intergrowth is enhanced as more fresh gel is supplied to the growing zeolite layer. Again, this is a reasonable result, since a higher renewal rate increases the average concentration of reactants in the synthesis gel. For sufficiently high renewal rates the system would approach the behavior of a continuous system operating at steady-state concentrations. On the other hand, lowering the renewal rate leads to a less efficient synthesis, as can also be seen in Table IV.3, where the two membranes prepared at the lowest renewal rate (1/25 min⁻¹) still present a large amount of defects after one synthesis cycle. Furthermore, Figure IV.22 shows that the trends outlined for both the weight gain and the N₂ permeance of the *as-synthesized* zeolite NaA layers can be also observed after 1 and 2 synthesis cycles.

IV.3.3.3. Effect of the seeding weight gain (SWG)

As it was discussed in section IV.3.2.3 for the synthesis of inner-side tubular zeolite NaA membranes under a centrifugal field and with a previous cross-flow filtration seeding, the SWG also seems to play a key role in the synthesis of inner-side membranes in the semi-continuous system. However, as shown in Table IV.3, no direct correlation exists between the SWG and the weight of zeolite gain after synthesis. For instance, membrane ZA-INN-SC-23

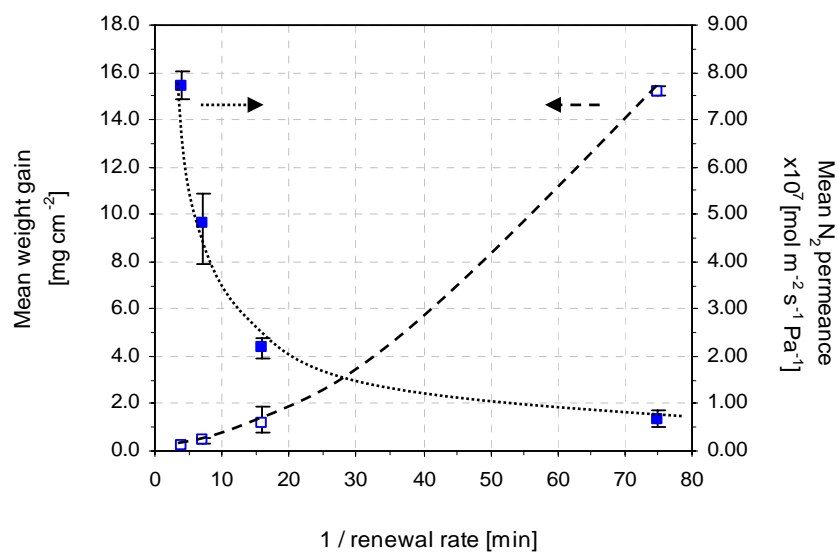


Figure IV.21: Evolution of the mean values of weight gain after synthesis and N₂ permeance with the renewal rate for inner-side tubular zeolite NaA membranes prepared in the semi-continuous system with arrangement III.8b in the autoclave. Synthesis conditions: SWG=0.10-0.29 mg cm⁻²; T=368 K; synthesis time=5 h; one synthesis cycle; renewal rate=1/16 min⁻¹). Dashed and dotted lines refer to the trends observed, respectively, for mean weight gain and N₂ permeance.

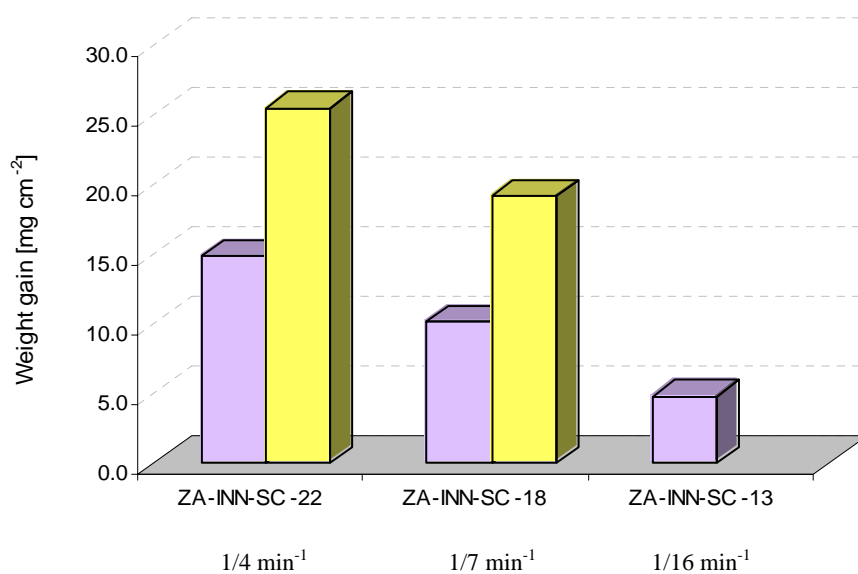


Figure IV.22: Evolution of the weight gain after synthesis with the renewal rate for three inner-side tubular zeolite NaA membranes prepared in the semi-continuous system with arrangement III.8b in the autoclave. Experimental conditions: SWG≈0.12-0.18 mg cm⁻². Other synthesis conditions as in Figure IV.21.

with a SWG of only 0.12 mg cm^{-2} gives rise to 9 mg cm^{-2} of zeolite material after the 1st synthesis cycle, while membrane ZA-INN-SC-21, with almost 5 times the SWG of membrane ZA-INN-SC-23, displays less than 6 mg cm^{-2} of zeolite weight after synthesis. The relationship between the SWG and the weight of the zeolite layer is more clearly presented in Figure IV.23 for membranes prepared with a variety of renewal rates and seeding techniques. It seems that, irrespective of the renewal rate used, the highest weights of the zeolite layer are obtained for SWG values lying in the range 0.10 and 0.20 mg cm^{-2} , which, according to the results listed in Table IV.3, appears to be strictly true for membranes prepared using the brush seeding method and also for those prepared by cross-flow filtration seeding followed by 2 synthesis cycles.

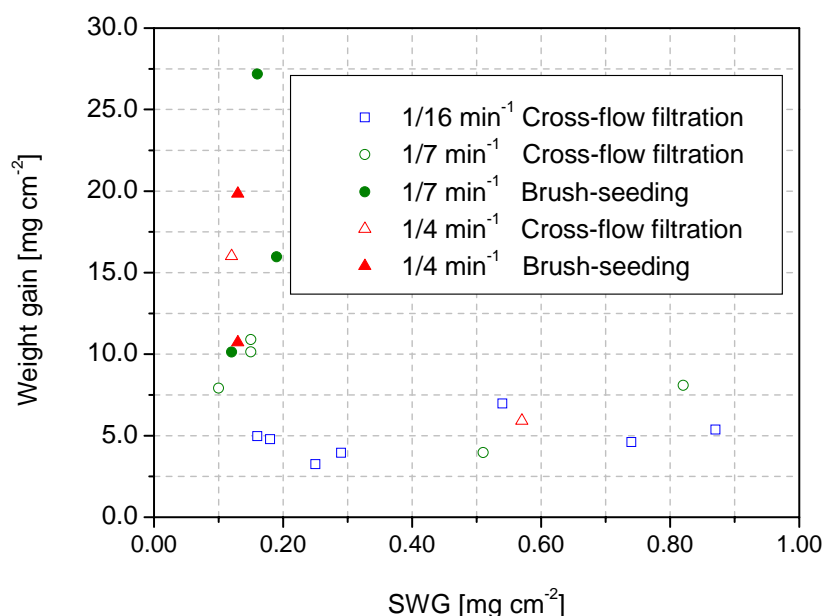


Figure IV.23: Relationship between the specific seeding weight gain (SWG) and the zeolite weight gained after one synthesis cycle in the semi-continuous system for the different membranes prepared in this work (arrangement III.8b in the autoclave, see Table IV.3).

It should be noted that these values are lower, though comparable, than the weight that would correspond to a monolayer of seeds (for 2 micron seeds and a zeolite density of 2.00 g cm^{-3} the weight of a monolayer of seeds would be around 0.25 mg cm^{-2} , assuming a void fraction of 0.30 in the monolayer). If the SWG is increased beyond 0.20 mg cm^{-2} , a rapid drop in the zeolite weight is observed, suggesting that multiple seed layers are unstable and may give rise to the detachment of lumps of seeds from the support surface either during membrane handling or as a consequence of the drag caused by the flow of the synthesis gel through the

lumen of the support. The detachment of these lumps from the support surface would produce seedless areas, giving rise to a lower overall weight gain after synthesis and to the presence of defects on the final membrane.

In agreement with these general comments, the N_2 permeance of the membranes synthesized with different renewal rates in the range $1/16$ - $1/4 \text{ min}^{-1}$ with a variety of renewal rates and seeding techniques also appears to depend on the SWG (see Figure IV.24). For instance, for renewal rates of $1/4 \text{ min}^{-1}$, the N_2 permeance increases around three orders of magnitude for a change in the SWG values from 0.12 to 0.60 mg cm^{-2} .

In light of the results obtained, the SWG seems to play a key role in the preparation of inner-side tubular membranes in the semi-continuous system. A minimum SWG around 0.15 - 0.50 mg cm^{-2} appears to be necessary for the further synthesis of well-intergrown zeolite layers, but higher values seem not to be recommendable. It should be noted that the general trends presented in this section for the weight gain and N_2 permeance after synthesis agree qualitatively with those reported in section IV.3.2 for the synthesis of inner-side tubular zeolite NaA membranes under a centrifugal field, where an optimum SWG value around 0.40 mg cm^{-2} was proposed according to the trends observed for the weight gain, N_2 permeance and He/N_2 ideal selectivity after synthesis with the SWG.

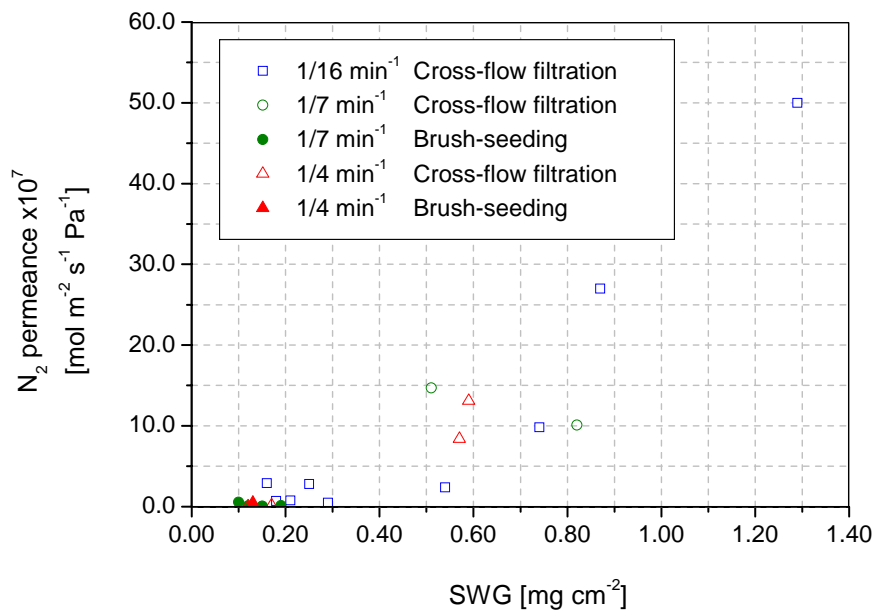


Figure IV.24: Evolution of the N_2 permeance with the SWG for inner-side tubular zeolite NaA membranes prepared in the semi-continuous system in one synthesis cycle (attachment III.8b in the autoclave, see Table IV.3).

IV.3.3.4. Preparation of inner-side tubular zeolite NaA membranes in a continuous system

Table IV.4 summarizes the main results concerning the weight gain and the N₂ permeance of zeolite NaA membranes synthesized on the inner side of tubular TiO₂ supports (rutile) in the continuous system described in section III.1.7. All the membranes were grown using gel 4 in one synthesis cycle in a metal tube that acted as autoclave at a gel flow rate of 1.5 mL min⁻¹ with or without a previous brush-seeding step. It should be highlighted that the weight gain of the membranes synthesized in 7 h with a previous brush-seeding lies in the range 3.5-8.5 mg cm⁻² (see Table IV.4), which is somewhat lower than that of the membranes synthesized in the semi-continuous system on the inner-side surface of α -alumina supports with the same gel in 1 synthesis cycle of 5 h, 5-20 mg cm⁻² (see Table IV.3). This difference in the weight gain of the *as*-synthesized membranes between both techniques might be ascribed to the lower temperature at which the continuous system operates, 353 K, compared to that of the semi-continuous system, 363-373 K.

Table IV.4: Synthesis conditions, weight gain after synthesis and nitrogen permeance for the membranes prepared in the continuous system (synthesis carried out at 353 K in 1 cycle; gel flow rate=1.5 mL min⁻¹).

<i>Membrane</i>	<i>Time (h)</i>	<i>SWG</i> [*] <i>[mg cm⁻²]</i>	<i>Weight gain</i> <i>[mg cm⁻²]</i>	<i>N₂ permeance</i> <i>[mol m⁻² s⁻¹ Pa⁻¹]</i>
ZA-INN-C-01	3	0.21	3.63	2.05 × 10 ⁻⁷
ZA-INN-C-02	3	0.13	8.22	3.70 × 10 ⁻⁸
ZA-INN-C-03	7	0.27	9.19	6.09 × 10 ⁻⁸
ZA-INN-C-04	7	0.11	4.70	4.45 × 10 ⁻⁷
ZA-INN-C-05	7	0.12	8.53	1.68 × 10 ⁻⁹
ZA-INN-C-06	7	0.00	3.51	1.00 × 10 ⁻⁵
ZA-INN-C-07	6	0.00	5.86	2.24 × 10 ⁻⁶
ZA-INN-C-08	7	0.00	7.24	2.04 × 10 ⁻⁸
ZA-INN-C-09	7	0.00	6.35	5.12 × 10 ⁻⁸

* The brush-seeding technique was used for the membranes synthesized by the secondary-growth method.

The lowest values of N₂ permeance for the *as*-synthesized membranes lie in the range 6-10 × 10⁻⁹ mol m⁻² s⁻¹ Pa⁻¹, which is very similar to that found for both outer- and inner-side tubular zeolite NaA membranes synthesized in the semi-continuous system that showed higher layer intergrowth. These results confirm the idea that gel renewal tends to improve the quality of the *as*-synthesized zeolite NaA layers. However, in light of the results obtained, for the membranes synthesized in the continuous system, higher layer intergrowth and thus lower

number of meso- and macroporous defects in the zeolite layer is obtained at lower weight gain values after synthesis, which reveals that this system is more efficient than the semi-continuous.

It should be stressed that, on the contrary to what is observed for the membranes prepared under a centrifugal field and in the semi-continuous system (see Tables IV.2 and IV.3), in light of the results exposed in Table IV.4, no clear trend between the weight gain and the SWG is observed. Nevertheless, the membranes synthesized with a previous brush-seeding show lower N_2 permeances (see Figure IV.25).

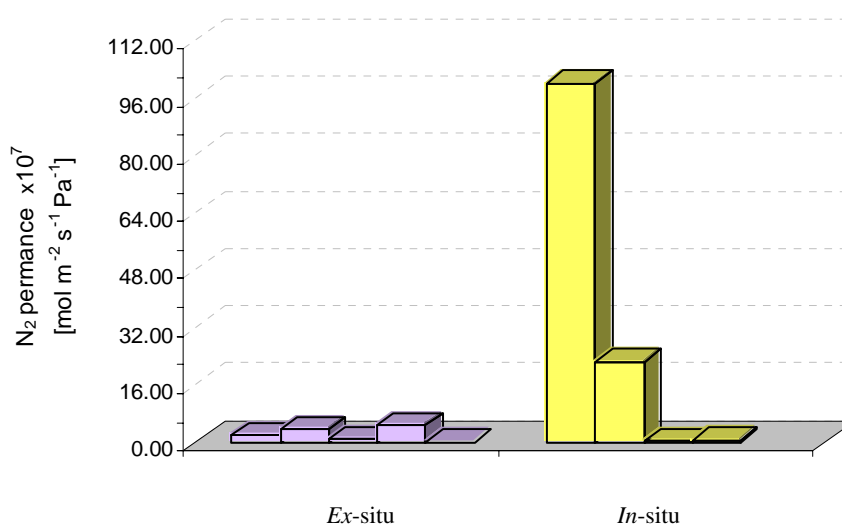


Figure IV.25: N_2 permeance of the inner-side zeolite NaA membranes after 1 synthesis cycle at 353 K and 6-7 h in the continuous system (gel flow rate=1.5 mL min⁻¹). For *ex-situ* membranes, the brush-seeding technique was used (SWG=0.11-0.27 mg cm⁻²).

IV.4. CHARACTERIZATION BY XRD AND SEM/EDS ANALYSES

IV.4.1. Characterization by XRD analyses

After the synthesis with the methods aforementioned in section IV.3, some of the *as*-synthesized composite tubular zeolite NaA membranes were broken for further XRD and SEM/EDS analyses. Figure IV.26 shows the XRD patterns of outer-side zeolite NaA membranes synthesized either with or without gel renewal in the semi-continuous system, while Figures IV.27, IV.28 and IV.29 show, respectively, the XRD patterns of inner-side membranes synthesized under a centrifugal field and in the semi-continuous and continuous systems. The effect of gel renewal in the crystallinity of the *as*-synthesized zeolite layers is

more explicitly shown in Figure IV.30. It should be emphasized that all the XRD patterns plotted in Figures IV.26-IV.29 reflect that zeolite NaA is the only zeolitic material present in the layers grown on the ceramic supports.

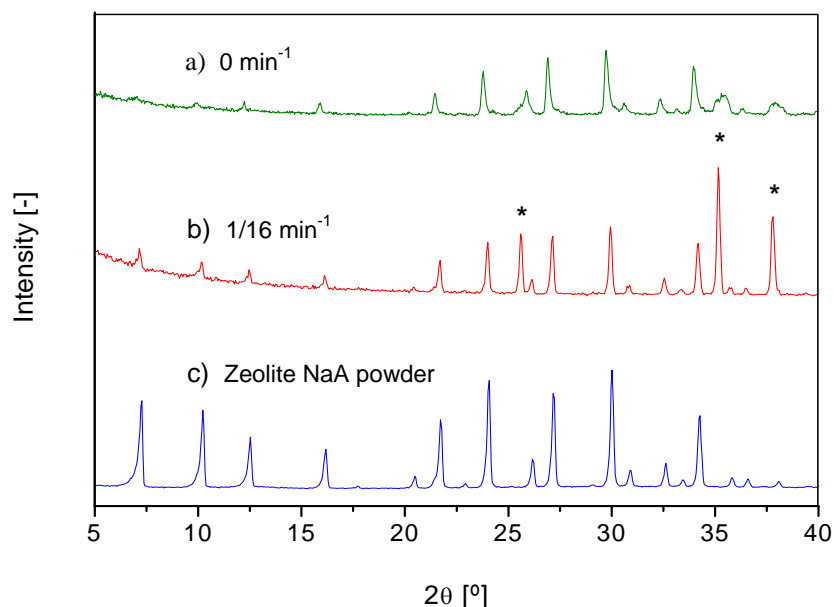


Figure IV.26: XRD patterns of zeolite NaA layers grown onto the outer-side of seeded α -alumina tubular supports (a) ZA-OUT-01, $T=373$ K, synthesis time=3 h, gel 2, 1 renewal rate= 0 min^{-1} , (b) ZA-OUT-SC-07, arrangement III.8b in the autoclave, $T=368$ K, synthesis time=5 h, gel 4, renewal rate= $1/16 \text{ min}^{-1}$; and (c) XRD pattern zeolite NaA powder obtained at the bottom of the glass vessel after the synthesis of membrane ZA-OUT-01. All the peaks correspond to zeolite NaA. The symbol (*) shows the location of α -alumina peaks from the support.

As can be seen in Figure IV.26, all the peaks in the XRD patterns of the *as*-synthesized outer-side zeolite NaA membranes ZA-OUT-01 and ZA-OUT-SC-07 prepared, respectively, statically in a glass vessel and in the semi-continuous system (renewal rate= $1/16 \text{ min}^{-1}$) agree fairly well with the XRD pattern obtained for the powder in the glass vessel after the 1st synthesis cycle of the former membrane for the range 5-40°. This agreement in angle position between the XRD patterns of the membranes and that of pure zeolite NaA powder reflects that zeolite NaA is the only zeolite material that crystallizes on the surface of the α -alumina tubular support. Furthermore, as can be also seen in Figure IV.26, the XRD pattern corresponding to membrane ZA-OUT-SC-07 shows narrower peaks and with higher intensity than those of membrane ZA-OUT-01. This result reveals that the zeolitic layer is more crystalline when the synthesis is carried out with gel renewal. A similar result can be observed

in Figure IV.27, where the XRD pattern of the inner-side zeolite NaA membrane ZA-INN-CF-02 prepared under a centrifugal field at a rotation speed of 100 r.p.m also shows narrower peaks and with higher intensity than those of inner-side membrane ZA-INN-01 prepared statically in a glass vessel. Hence, the presence of a centrifugal field in the synthesis of appears to allow the growth of zeolite NaA layers with higher crystallinity.

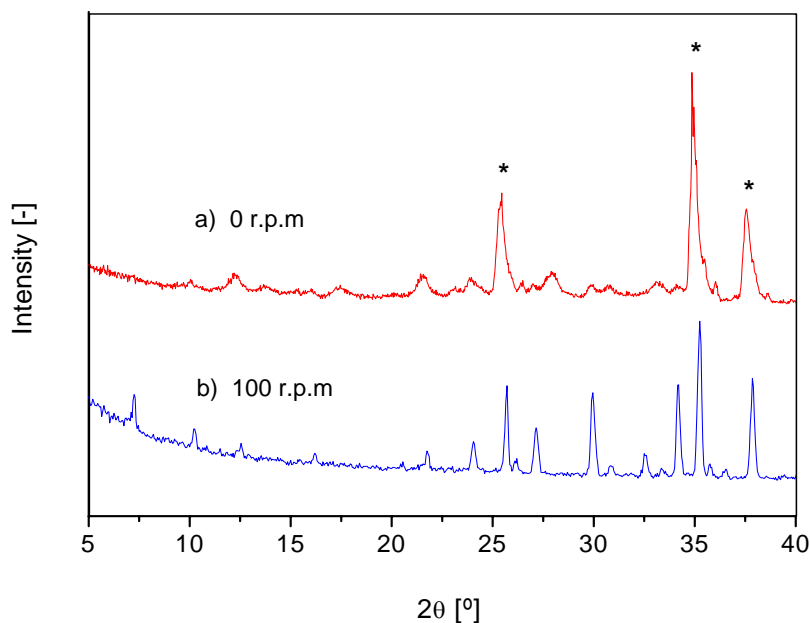


Figure IV.27: XRD patterns of zeolite NaA layers grown onto the inner-side of seeded α -alumina tubular supports (a) ZA-INN-01, SWG=0.15 mg cm⁻²; ω =0 r.p.m; (b) ZA-INN-CF-02, SWG=0.20 mg cm⁻²; ω =100 r.p.m. Other synthesis conditions: T=373 K, synthesis time=3 h, gel 1. The symbol (*) shows the location of α -alumina peaks from the support.

Furthermore, for the assessment of the crystalline character of the membrane layers synthesized in the semi-continuous system, membranes with similar SWG under the same synthesis conditions but different renewal rates were selected. The XRD patterns of membranes ZA-INN-SC-29, ZA-INN-SC-26 and ZA-INN-SC-08 prepared under the same synthesis conditions with renewal rates of 1/4, 1/7 and 1/16 min⁻¹, respectively, are plotted in Figure IV.28. For all these membranes, pure zeolite NaA was the only zeolitic phase present on the support. Peaks corresponding to the α -alumina support can also be observed. The XRD patterns indicate a higher crystallinity for membrane ZA-INN-SC-29 (1/4 min⁻¹ renewal rate), and lowest for membrane ZA-INN-SC-08 (1/16 min⁻¹), thus indicating that an increase in the renewal rate leads to a more crystalline zeolite NaA layer.

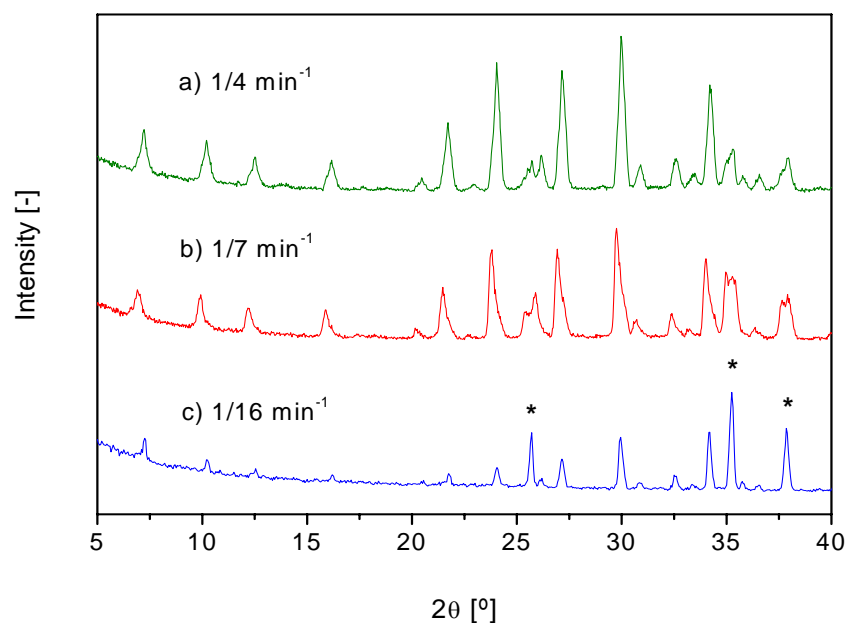


Figure IV.28: XRD patterns of zeolite NaA layers grown onto the inner-side of seeded α -alumina tubular supports in the semi-continuous system. (a) Membrane ZA-INN-SC-29, renewal rate= $1/4 \text{ min}^{-1}$; (b) Membrane ZA-INN-SC-26, renewal rate= $1/7 \text{ min}^{-1}$; (c) Membrane ZA-INN-SC-08, renewal rate= $1/16 \text{ min}^{-1}$. Synthesis conditions: SWG= $0.12\text{-}0.25 \text{ mg cm}^{-2}$, arrangement III.8b in the autoclave, $T=368 \text{ K}$, synthesis time= 5 h , 2 cycles. The symbol (*) shows the location of α -alumina peaks from the support.

Figure IV.29 shows the XRD patterns of the inner-side zeolite NaA membranes ZA-INN-C-02, ZA-INN-C-04 and ZA-INN-C-07 prepared in the continuous system. As can be seen, the intensity of the peaks related to zeolite NaA of membranes ZA-INN-C-04 and ZA-INN-C-07 is higher than that corresponding to membrane ZA-INN-C-02. Furthermore, the peaks corresponding to titania support are less intense for the former membranes. These observations might be accounted for by the higher layer thickness of membranes ZA-INN-C-04 and ZA-INN-C-07, since they were synthesized at longer synthesis times (7 vs. 3 h). On the other hand, the XRD pattern of membrane ZA-INN-C-04 prepared by the *ex-situ* method with a previous brush-seeding step, shows higher and more definite peaks than that of membrane ZA-INN-C-07 prepared without a previous seeding step. Accordingly, the seeding of the support appears to allow the synthesis of more crystalline zeolite layers due to a more uniform and controlled growth of the zeolite material. Finally, a summary of the effect of gel renewal in the crystallinity of the zeolite layers synthesized with the different methods outlined in this work is shown in Figure IV.30. As can be seen, the XRD pattern of membranes prepared in the semi-

continuous system show the highest crystallinity, since the related peaks show the highest intensities.

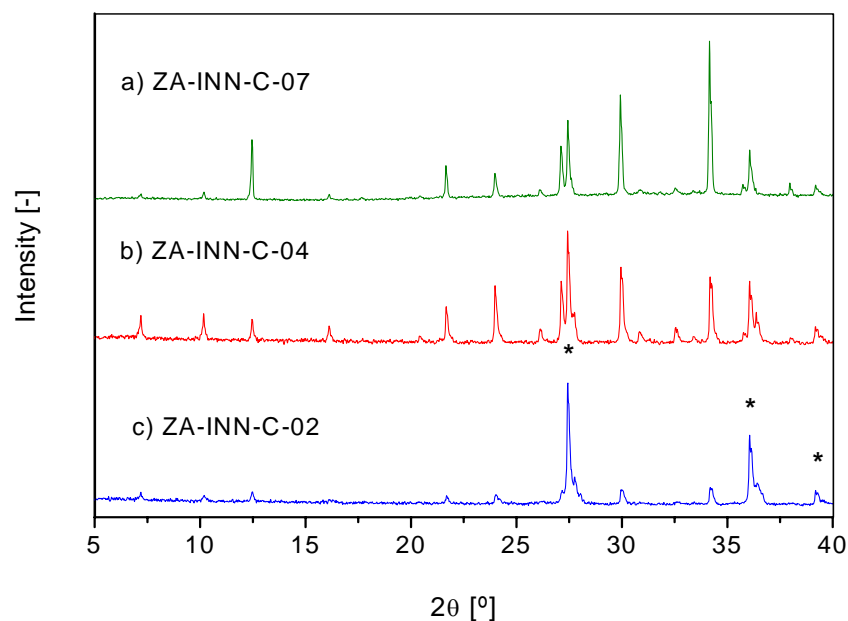


Figure IV.29: XRD patterns of zeolite NaA layers grown onto the inner-side of seeded α -alumina tubular supports in the continuous system (a) Membrane ZA-INN-C-02, SWG=0.13 mg cm⁻²; (b) Membrane ZA-INN-C-04, SWG=0.11 mg cm⁻²; (c) Membrane ZA-INN-C-07, SWG=0.00 mg cm⁻². Other synthesis conditions: gel flow rate=1.5 mL min⁻¹, T=353 K, synthesis time=6-7 h, gel 4. The symbol (*) shows the location of TiO₂ (rutile) peaks from the support.

IV.4.2. Characterization by SEM/EDS analyses

Figures IV.31-IV.39 show some scanning electron micrographs (SEM) corresponding to unseeded and seeded supports with cross-flow filtration seeding and to outer- and inner-side zeolite NaA layers synthesized in this work.

IV.4.2.1. Seeded and unseeded supports

Figure IV.31 shows the top view scanning electron micrographs (SEM) corresponding to unseeded and seeded α -alumina supports with cross-flow filtration technique. Figure IV.31a shows the SEM micrograph of an α -alumina support (mean pore size, 1.9 μ m) prepared by pressing α -alumina particles of a size around 5-10 μ m, where macropores around 2 μ m can be clearly observed. On the other hand, Figures IV.31b shows the top view

micrograph of a support seeded at low SWG ($<0.40 \text{ mg cm}^{-2}$), where it can be clearly observed that most of the particles agglomerate in particular zones of the support, which might correspond to the macropores of the solid. This agglomeration in the macropores of the support would be responsible for the reduction of the water permeability described in Figure IV.4 in the cross-flow seeding process, as the macropores are progressively blocked by the zeolite seeds.

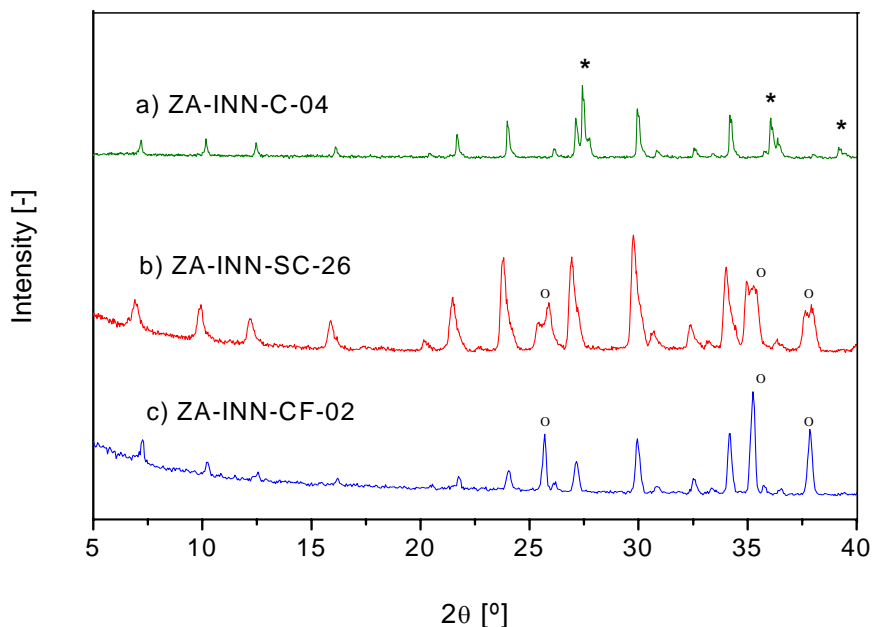


Figure IV.30: XRD patterns of zeolite NaA layers grown onto the inner-side of seeded α -alumina tubular supports prepared with $\text{SWG}=0.12\text{-}0.15 \text{ mg cm}^{-2}$ and synthesized in (a) continuous system, gel flow rate= 1.5 mL min^{-1} ; (b) semi-continuous system, renewal rate= $1/7 \text{ min}^{-1}$; (c) glass vessel in a centrifugal field, $\omega=100 \text{ r.p.m.}$ Synthesis conditions as in Figures IV.27-IV.29. The symbols (*) and (o) show, respectively, the location of TiO_2 (rutile) and α -alumina peaks from the supports.

IV.4.2.2. Outer-side zeolite NaA membranes prepared in the semi-continuous system

Figure IV.32 shows the top view and cross-section SEM micrographs of the outer-side membrane ZA-OUT-SC-07 synthesized in the semi-continuous system with a renewal rate of $1/16 \text{ min}^{-1}$. The inspection of the top view SEM micrograph of this membrane (see Figure IV.32a) shows the presence of a randomly oriented distribution of cubic zeolite crystals. Moreover, the inspection of the cross-flow SEM micrograph (see Figure IV.32b) reveals the presence of a continuous and well-intergrowth layer of a thickness about $10 \mu\text{m}$.

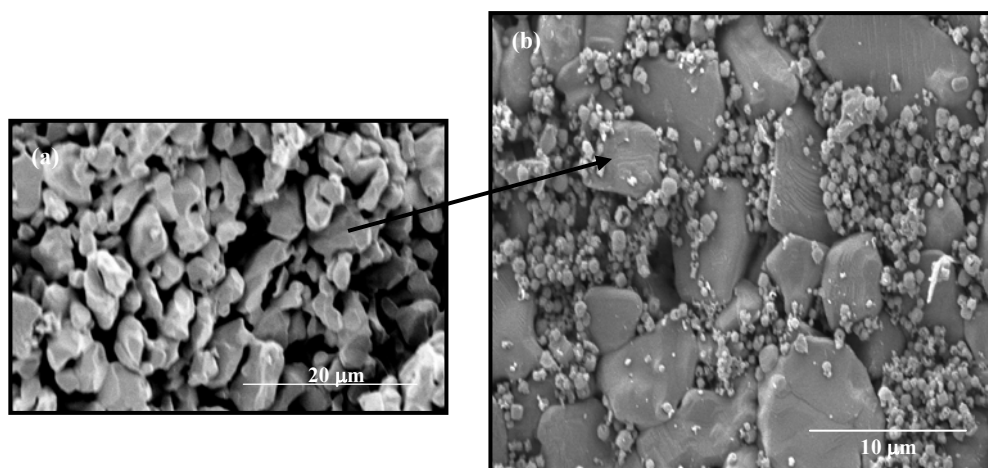


Figure IV.31: Top view SEM micrographs of (a) an unseeded clean α -alumina support; (b) seeded support by the cross-flow seeding technique with $\text{SWG}=0.38 \text{ mg cm}^{-2}$ (feed flow rate= 5.5 L min^{-1} ; mean particle size, $7 \text{ }\mu\text{m}$; $\text{pH}=8.0$; $\Delta P_m=1.0 \text{ bar}$).

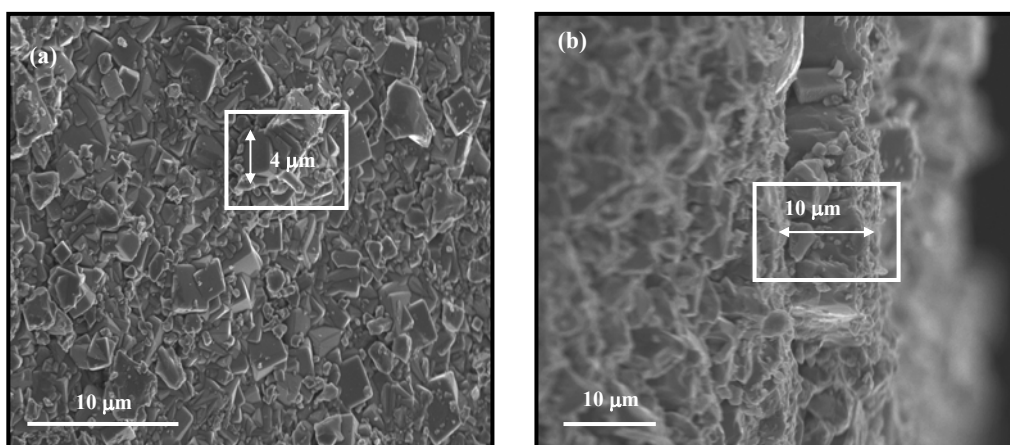


Figure IV.32: SEM micrographs of membrane ZA-OUT-SC-07 ($\text{SWG}=0.46 \text{ mg cm}^{-2}$; renewal rate= $1/16 \text{ min}^{-1}$). (a) Top view; (b) Cross-section.

IV.4.2.3. Inner-side zeolite NaA membranes prepared under a centrifugal field

Figures IV.33a-d show the SEM micrographs of the inner-side zeolite NaA membrane ZA-INN-CF-02 prepared under a centrifugal field in 3 synthesis cycles. The inspection of the top view micrograph of this membrane (see Figure IV.33a-b) reveals the presence of randomly oriented cubic crystals typical of zeolite A up to $5 \text{ }\mu\text{m}$ in size in a continuous well-intergrown top layer of thickness around $30 \text{ }\mu\text{m}$ (see Figures IV.33c). Although some apparent intercrystalline porosity is observed in Figure IV.33a, this might be only regarded as *dead-end*

porosity, that is, they might not actually play a role as defects for this membrane taking into account the He/N₂ selectivities approaching the ideal Knudsen value. In fact, on the grounds of the high intergrowth that this membrane shows, zeolite A crystals might have crystallized underneath these pores that might remove their potential negative effect in the final performance of the membrane.

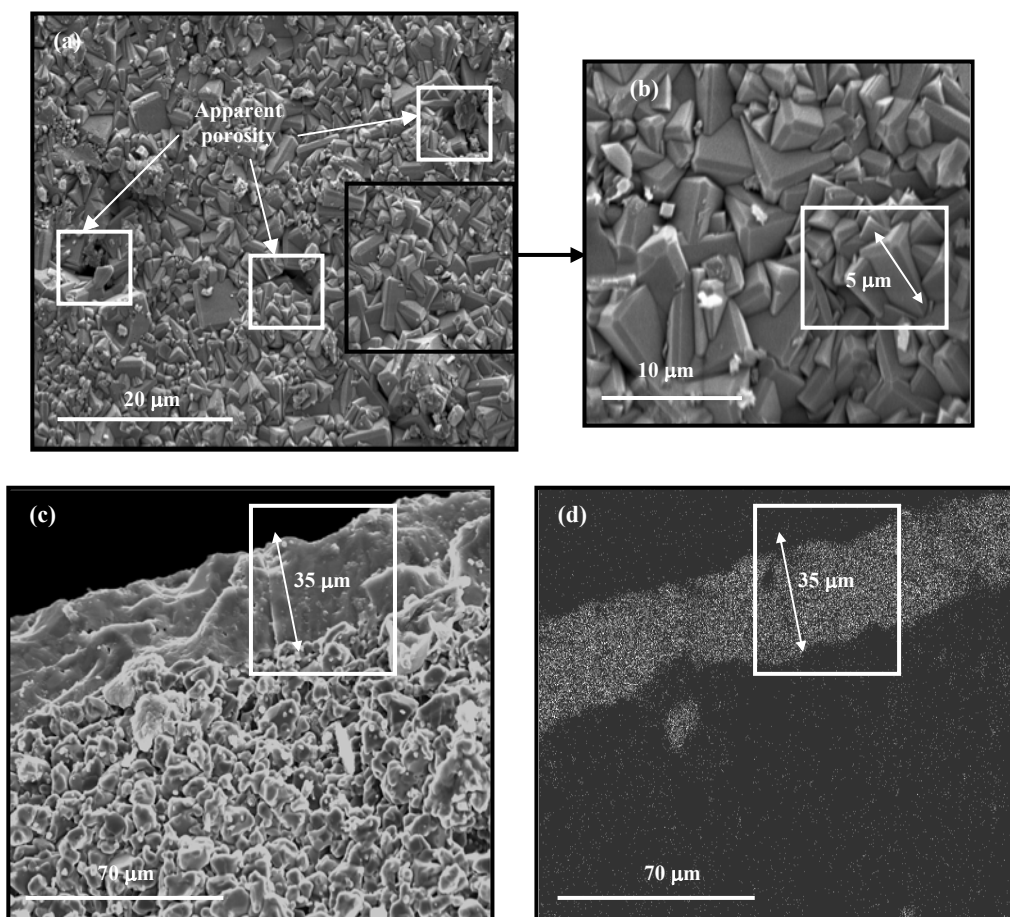


Figure IV.33: SEM micrographs of membrane ZA-INN-CF-02 (SWG=0.20 mg cm⁻²; ω =100 r.p.m; T = 373 K; 3 synthesis cycles with gel 1. (a) and (b) Top views; (c) Cross-section; (d) Si mapping of the cross-section.

Furthermore, regarding the the Si-mapping (EDS microanalysis) of the cross-section of the membrane (see Figure IV.33d), all the zeolite material seems to be only present in the synthesized zeolite layer, that is, no zeolitic material is found in the macropores of the support. This result indicates that the synthesis gel does not appear to have penetrated the macropores of the support during the synthesis of the membrane.

IV.4.2.4. Inner-side zeolite NaA membranes prepared in the semi-continuous system

The SEM micrographs of membranes ZA-INN-SC-08, ZA-INN-SC-19 and ZA-INN-SC-28 prepared, the former two, with a cross-flow filtration seeding technique and with 1/16 and 1/7 min⁻¹ renewal rates, and the latter with a brush-seeding technique and with a renewal rate of 1/4 min⁻¹ are shown in Figure IV.34. The inspection of the top view micrographs of these membranes (see Figures IV.34a,c,e) shows in all cases well-crystallized material typical of A-type zeolite, with cubic and truncated-side cubic crystals. The kind of seeding (i.e. brush-seeding or cross-flow filtration) does not seem to influence the mean crystal size or thickness of the layer. However, a cleaner surface can be observed for membrane ZA-INN-SC-28, prepared with a renewal rate of 1/4 min⁻¹, which is consistent with the higher crystallinity of the XRD patterns observed for the membranes prepared at higher renewal rates (see Figure IV.29). The cross-section micrographs of membranes prepared at higher renewal rates (1/7 and 1/4 min⁻¹, see Figures IV.34d,f), show a similar appearance, regarding both the morphology and thickness of the zeolite layers. On the other hand, the SEM observations of membranes with both types of seeding indicate that, using both seeding methods, approximately the same crystal size and thickness was obtained for the *as*-synthesized membranes, provided that the SWG was similar. However, for 1/16 min⁻¹ renewal rate (see Figure IV.34b) the cross-section images shows some non-continuous domains which would account for the excess N₂ permeances given in Table IV.5 for this membrane.

Table IV.5: Thickness of some inner-side membranes prepared in the semi-continuous system (membranes synthesized with gel 4 in 2 cycles)

<i>Membrane</i>	<i>Seeding method</i>	<i>Arrangement (Figure III.8)²</i>	<i>Renewal rate [min⁻¹]</i>	<i>N₂ permeance [mol m⁻² s⁻¹ Pa⁻¹]</i>	<i>Layer thickness [μm]</i>
ZA-INN-SC -08	Filtration	c	1/16	2.45 x 10 ⁻⁷	10
ZA-INN-SC -19	Filtration	b	1/7	3.65 x 10 ⁻⁹	20
ZA-INN-SC -28	Brush	b	1/4	<1.00 x 10 ⁻⁹	20

IV.4.2.5. Inner-side zeolite NaA membranes prepared in the continuous system

Figures IV.35, IV.36 and IV.37 show the SEM micrographs of membranes ZA-INN-C-02, ZA-INN-C-04 and ZA-INN-C-07 synthesized in the continuous system. The inspection of the top view micrographs of these membranes (see Figures IV.35a-b-IV.37a-b) reveals in all cases the presence of well-intergrown layers constituted by a randomly oriented distribution of cubic and truncated-side cubic crystals. Figures IV.35a and IV.37b also show the presence of zeolite NaA cubic-truncated crystals up to 10-12 μm in size dispersed on a compact and

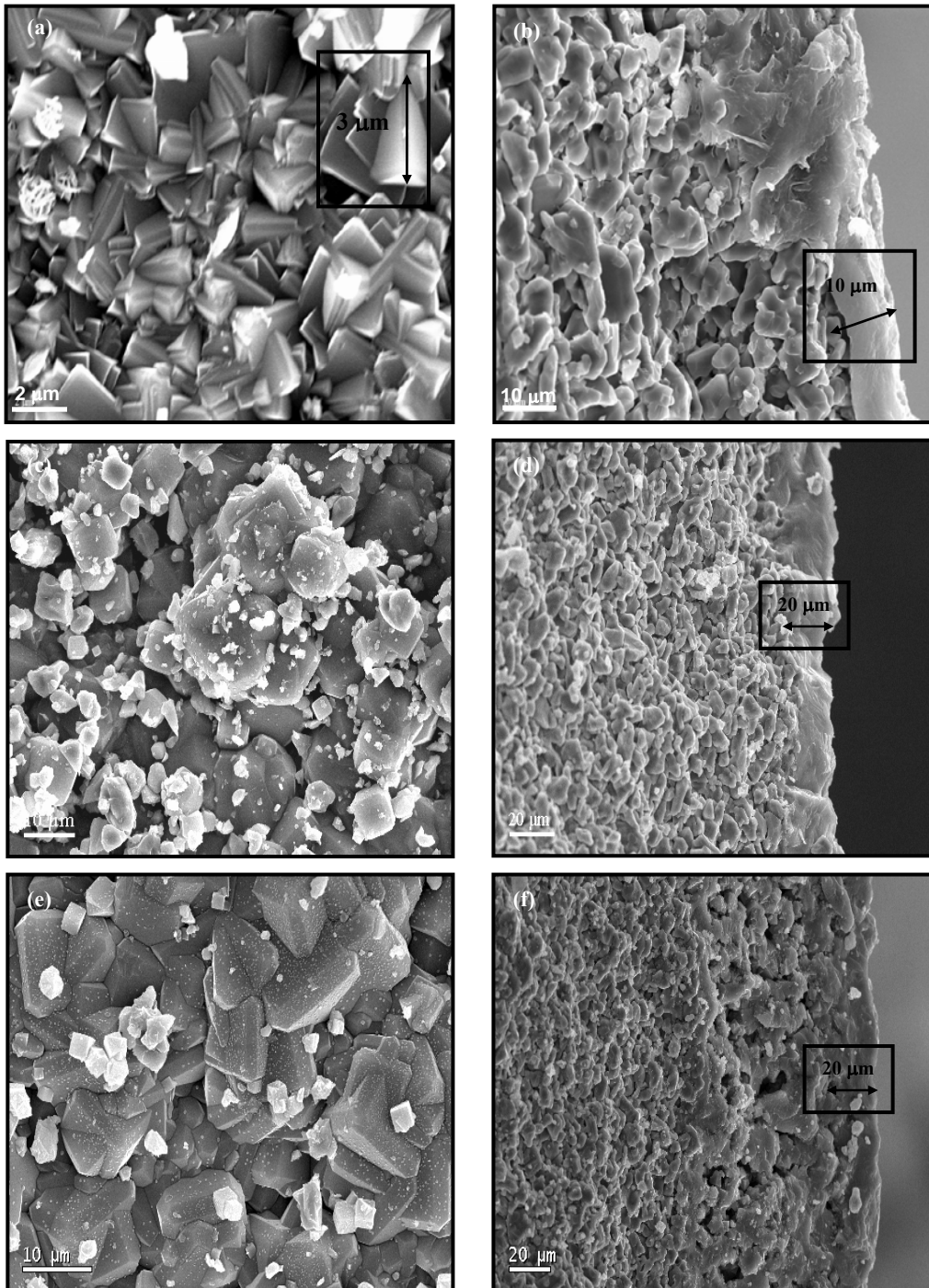


Figure IV.34: SEM micrographs of membranes (a, b) ZA-INN-SC-08 (cross-flow filtration seeding, $\text{SWG}=0.25 \text{ mg cm}^{-2}$; renewal rate= $1/16 \text{ min}^{-1}$), (c, d) ZA-INN-SC-19 (cross-flow filtration seeding, $\text{SWG}=0.15 \text{ mg cm}^{-2}$; renewal rate= $1/7 \text{ min}^{-1}$) and (e, f) ZA-INN-SC-28 (brush-seeding, $\text{SWG}=0.13 \text{ mg cm}^{-2}$; renewal rate= $1/4 \text{ min}^{-1}$). Synthesis conditions: arrangement III.8b in the autoclave, $T=368 \text{ K}$, 2 synthesis cycles, gel 4. Top views (a), (c) and (e); Cross-sections (b), (d) and (f).

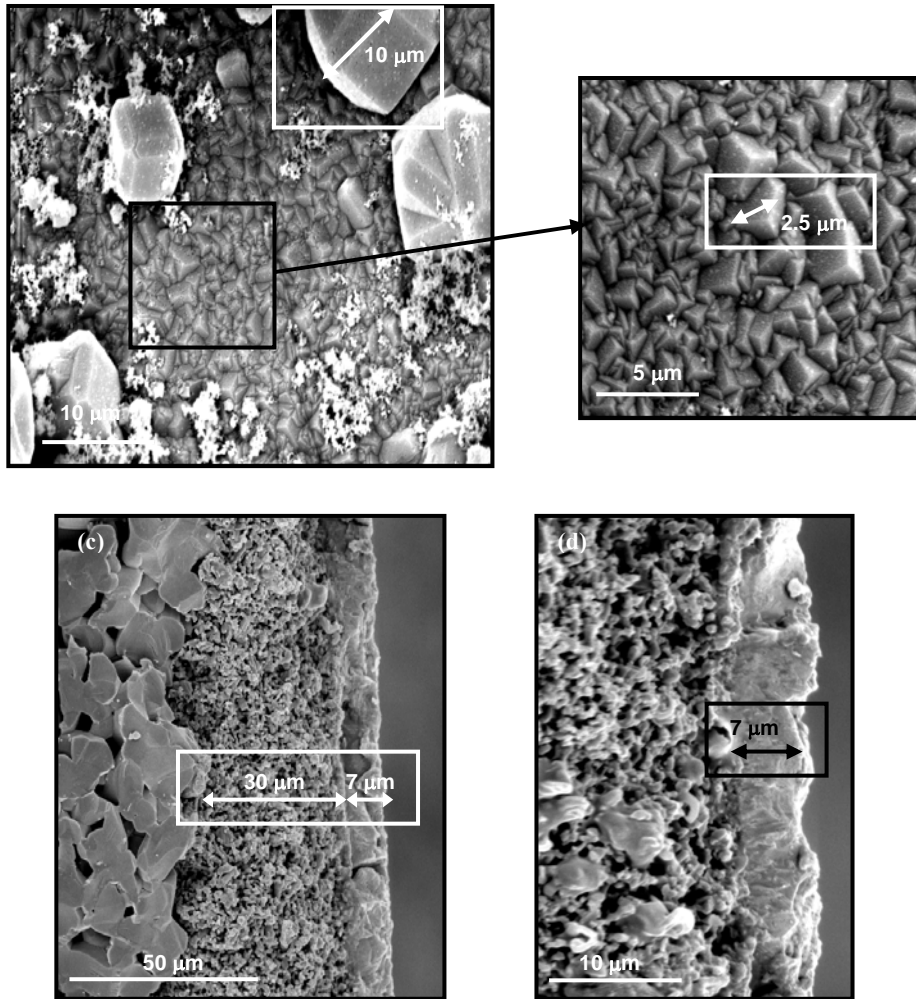


Figure IV.35: SEM micrographs of membrane ZA-INN-C-02. (a) y (b) Top view; (c) y (d) Cross-sections. Micrographs (b) and (d) are magnifications of (a) and (c), respectively. Synthesis conditions: SWG=0.13 mg cm⁻², 1 synthesis cycle, gel flow rate= 1.5 mL min⁻¹, T=353 K, synthesis time=6 h, gel 4.

intergrown layer of zeolite NaA crystals of smaller size. On the other hand, the cross-section micrographs of these membranes (see Figures IV.35c-d, IV.36c-d and IV.37c) show the formation of well-intergrown zeolite NaA layers of 7-20 μm in thickness. Three layers can be clearly observed (see Figure IV.35c): (1) synthesized zeolite layer; (2) intermediate TiO₂ layer (mean pore size, ~1 μm; thickness, ~30 μm); and (3) TiO₂ bulk support constituted by large TiO₂ crystals (mean size, ~25 μm) that generate macropores of a mean size of ~7 μm.

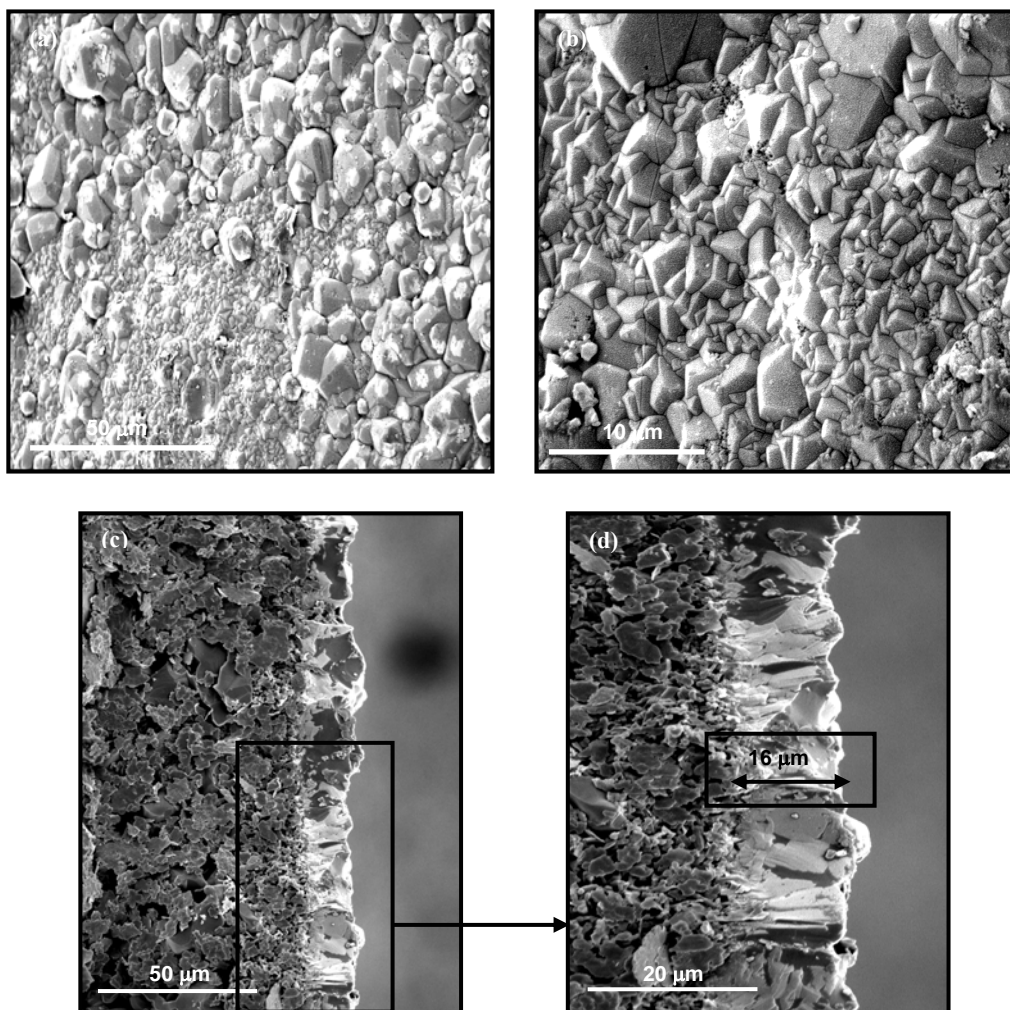


Figure IV.36: SEM micrographs of membrane ZA-INN-C-04. (a) y (b) Top view; (c) y (d) Cross-section. Micrograph (d) is a magnification of (c). Synthesis conditions: SWG=0.11 mg cm⁻², 1 synthesis cycle, gel flow rate= 1.5 mL min⁻¹, T=353 K, synthesis time=7 h, gel 4.

On the other hand, no morphological differences are observed in the top view SEM micrograph of membrane ZA-INN-C-04 (see Figures IV.36a-b) prepared by the *ex situ* method (brush-seeding, SWG=0.13 mg cm⁻²) than that of membrane ZA-INN-C-07 (see Figures IV.37a-b) prepared by the *in situ* method, that is, without a previous seeding step. Therefore, the seeding of the support prior to the synthesis with a gel does not seem to exert any influence on the final morphology of the synthesized zeolite layers.

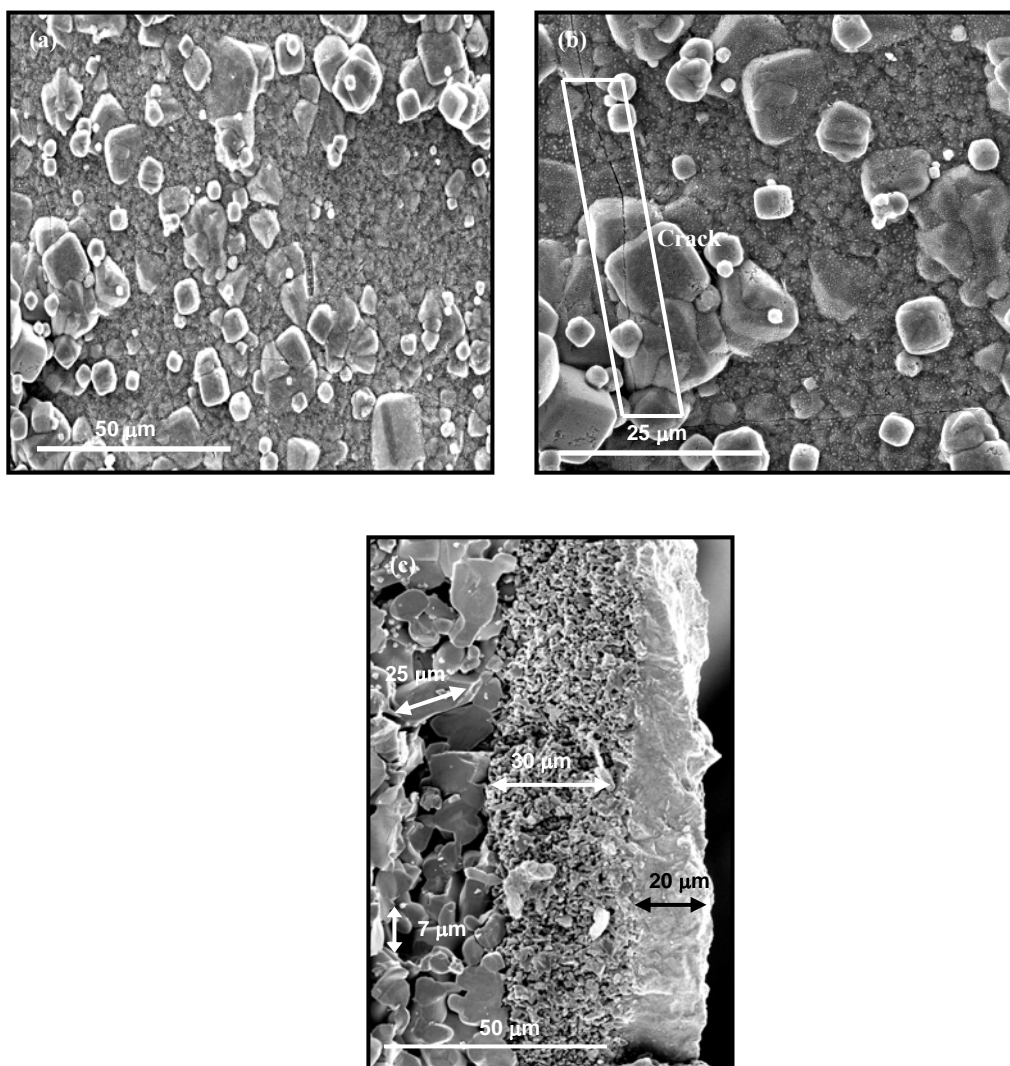


Figure IV.37: SEM micrographs of membrane ZA-INN-C-07. (a) y (b) Top view; (c) Cross-section. A crack can be observed in the top view micrographs. Synthesis conditions: SWG=0 mg cm⁻², 1 synthesis cycle, gel flow rate= 1.5 mL min⁻¹, T=353 K, synthesis time=6 h, gel 4.

A most thorough inspection of the top view micrographs of membrane ZA-INN-C-07 (see Figures IV.37a-b) reveals the presence of some fissures or cracks in the zeolite layer, which might account for the higher N₂ permeance measured for this membrane compared to those of membranes ZA-INN-C-02 and ZA-INN-C-04, where no cracks in their top view micrographs are observed. The presence of cracks in the zeolite layer of the former membrane might be ascribed to the thermal stress that zeolite layers might suffer during the post-treatment step of their preparation on the grounds of the difference between the thermal expansion coefficients of the zeolite layer and that of the TiO₂ support.

IV.5. PV PERFORMANCE OF THE AS-SYNTHEZIZED MEMBRANES

The aim to separate of ethanol/water liquid mixtures with high production by means of vacuum pervaporation (VPV) constitutes the final application of the membranes synthesized in this work. All the membranes synthesized in this study were tested to assess the most appropriate method suitable for their preparation. In this section, the results concerning the dehydration of ethanol/water liquid mixtures with VPV are shown and discussed. The results in the PV have been correlated with SWG values, weight gain, N₂ permeance and He/N₂ selectivity in order to predict the pervaporative performance of a membrane without the need to carry out any experiments and their reproducibility has been a subject of special interest. Finally, the results obtained for pervaporation have been also compared with those obtained in a distillation process.

IV.5.1. Summary of VPV results

The results for the VPV of ethanol/liquid liquid mixtures for the membranes prepared in this work are summarized in Tables IV.6 and IV.7. Table IV.6 lists the PV data concerning the outer-side tubular zeolite NaA membranes prepared statically in a glass vessel and in the semi-continuous system, while Table IV.7 lists the PV performance of the inner-side tubular zeolite NaA membranes prepared in this work, which is divided into three parts: (1) membranes synthesized in a glass vessel either with or without the presence of a centrifugal field; (2) membranes synthesized in the semi-continuous system; and (3) membranes synthesized in the continuous system.

Table IV.6: Conditions and results of the VPV study of the outer-side tubular zeolite NaA membranes prepared in this work (feed pressure=1-3 bar and permeate pressure<2 mbar for all the experiments).

<i>Membrane</i>	<i>T [K]</i>	<i>X_w (feed) [wt. %]</i>	<i>Y_w (permeate) [wt. %]</i>	<i>α_{w/E} [-]</i>	<i>N^T [kg m⁻² h⁻¹]</i>
ZA-OUT-01	322.4	7.65	75.12	36	0.34
ZA-OUT-02	322.4	6.32	83.20	73	0.18
ZA-OUT-SC -01	373-379	12.11	95.73	163	3.80
ZA-OUT-SC -02	373-379	12.45	99.47	1310	3.12
ZA-OUT-SC -03	373-379	11.34	95.14	153	2.11
ZA-OUT-SC -04	373-379	10.21	98.37	530	4.70
ZA-OUT-SC -08	373-379	10.12	97.80	394	3.50

Table IV.7: Conditions and results of the VPV study of the inner-side tubular zeolite NaA membranes prepared in this work (feed pressure=1-3 bar and permeate pressure<2 mbar for all the experiments).

<i>Membrane</i>	<i>T [K]</i>	<i>X_w (feed) [wt. %]</i>	<i>Y_w (permeate) [wt. %]</i>	<i>α_{w/E} [-] *</i>	<i>N^T [kg m⁻² h⁻¹]^{2**}</i>
ZA-INN-CF -01	323.0	6.67	97.41	502	0.62
ZA-INN-CF -02	323.0	5.66	93.35	237	0.43
ZA-INN-CF -03	324.0	8.11	98.11	294	0.39
ZA-INN-CF -04	324.0	8.12	97.48	437	0.51
ZA-INN-CF -05	323.0	8.22	92.34	154	0.62
ZA-INN-CF -06	323.0	8.25	88.23	73	0.52
ZA-INN-CF -07	323.0	12.13	32.73	3	1.45
ZA-INN-CF -08	324.0	6.20	12.00	2	1.85
ZA-INN-CF -09	323.0	5.84	22.47	56	0.17
ZA-INN-CF -10	323.0	5.11	11.87	3	1.57
ZA-INN-01	324.0	7.19	14.57	2	2.15
ZA-INN-SC -01	323.5	8.00	14.78	2	2.34
ZA-INN-SC -02	323.5	8.00	30.23	5	1.62
ZA-INN-SC -03	327.5	8.00	30.24	5	3.94
ZA-INN-SC -04	324.4	16.98	35.55	3	1.32
ZA-INN-SC -05	323.5	7.98	14.65	2	2.81
ZA-INN-SC -06	324.4	7.98	26.71	2	1.75
ZA-INN-SC -07	323.4	7.98	37.77	7	1.11
ZA-INN-SC -08	323.2	16.98	33.34	2	2.97
ZA-INN-SC -09	323.2	10.36	26.74	3	1.82
ZA-INN-02	324.0	10.23	25.43	2	2.20
ZA-INN-SC -12	323.4	7.98	20.64	3	2.45
ZA-INN-SC -13	325.0	7.98	26.69	4	2.31
ZA-INN-SC -14	323.6	7.98	30.23	5	1.51
ZA-INN-SC -15	324.9	7.98	26.81	2	3.05
ZA-INN-SC -16	325.0	7.98	20.64	3	2.51
ZA-INN-SC -17	325.3	7.98	25.74	4	2.48
ZA-INN-SC -18	333.1	9.92	99.00	1050	0.49

Table IV.7 (to be continued)

ZA-INN-SC -19	323.2	10.36	26.74	3	1.78
ZA-INN-SC -20	327.1	9.92	84.83	51	0.93
ZA-INN-SC -21	325.3	7.98	20.64	3	1.51
ZA-INN-SC -22	331.3	9.92	93.32	127	0.85
ZA-INN-SC -23	327.9	16.01	98.38	317	0.83
ZA-INN-SC -24	326.4	10.07	96.35	289	0.46
ZA-INN-SC -25	329.0	10.07	99.24	1168	0.57
ZA-INN-SC -26	324.3	10.21	99.64	2444	0.47
ZA-INN-SC -27	325.2	8.38	83.12	54	0.57
ZA-INN-SC -28	330.0	8.38	99.93	16222	0.43
ZA-INN-SC -29	327.1	9.92	97.66	379	0.31
ZA-INN-C-01	323.2	8.38	81.39	51	0.93
ZA-INN-C-02	323.2	8.38	26.64	4	>1.00
ZA-INN-C-03	323.2	8.38	98.90	1091	0.76
ZA-INN-C-04	323.2	8.38	97.69	495	1.16
ZA-INN-C-05	323.2	8.38	99.84	8538	0.83
ZA-INN-C-06	323.2	8.38	29.98	5	>1.00
ZA-INN-C-07	323.2	8.38	46.14	10	>1.00
ZA-INN-C-08	323.2	8.38	93.28	160	0.72
ZA-INN-C-09	323.2	8.38	86.87	76	0.97

¹Standard deviation <10% for all the experiments

²Standard deviation <5% for all the experiments

The evolution of the total flux across of the membrane, N^T [$\text{kg m}^{-2} \text{h}^{-1}$], with the water/ethanol selectivity [-] for all the inner-side zeolite NaA membranes tested in pervaporation is plotted in Figure IV.38. As can be observed, for lower total fluxes, higher water/ethanol selectivities are obtained, which means that the separation of water is enhanced on the basis of the hydrophilic character of zeolite NaA crystals that promotes the selective adsorption of water and further surface diffusion through them. Otherwise, an increase in the total flux involves lower water/ethanol selectivities due to a higher number of meso- and macroporous defects in the zeolite NaA layers. Therefore, according to Figure IV.38, the order of magnitude of the PV total flux across a zeolite membrane seems to provide significant

information concerning the number of defects of the layers, and thus, to allow the prediction of the order of magnitude of the selectivity towards water separation.

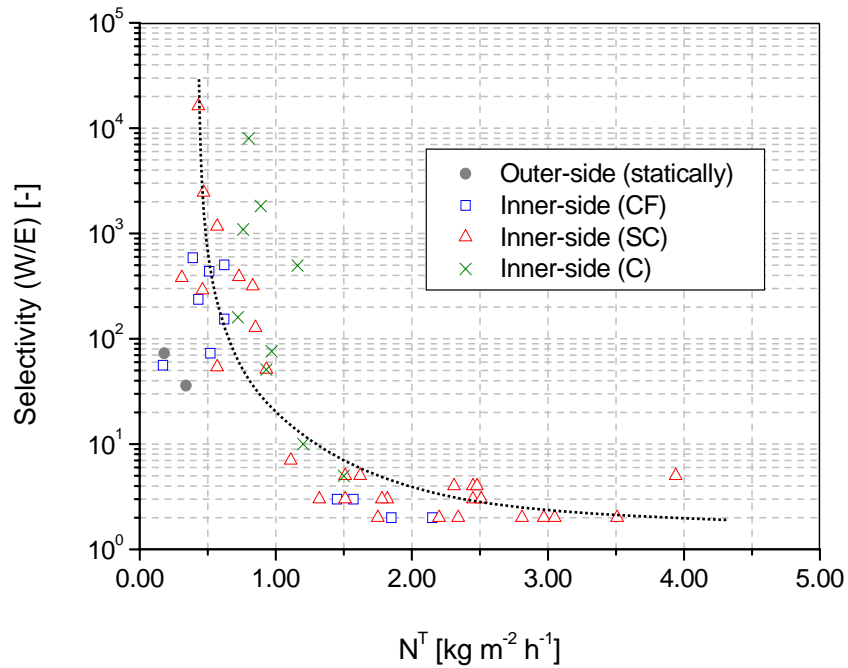


Figure IV.38: Evolution of the selectivity (W/E) with the total flux in the PV experiments for the outer- and inner-side zeolite NaA membranes synthesized in this work. Synthesis conditions in Table IV.3. PV conditions as in Tables IV.6 and IV.7. The dotted line refers to the trend observed.

IV.5.2. Effect of the N_2 permeance and He/N_2 ideal selectivity

Figures IV.39 and IV.40 show the effect of N_2 permeance in both the water/ethanol selectivity and the total flux for all the membranes listed in Tables IV.6 and IV.7 for different SWG values and synthesis conditions. As can be seen in Figure IV.39, the water/ethanol selectivity tends to increase with a decrease in the N_2 permeance, while the total flux across the membrane shows the opposite trend. In agreement with the above discussion on the relationship between N_2 permeance and membrane quality, it can be seen that the membranes are able to separate effectively ethanol/water mixtures (selectivity towards water separation of 100 and above) only when their N_2 permeance is in the range of $2 \times 10^{-8} \text{ mol m}^{-2} \text{ s}^{-1} \text{ Pa}^{-1}$ and below.

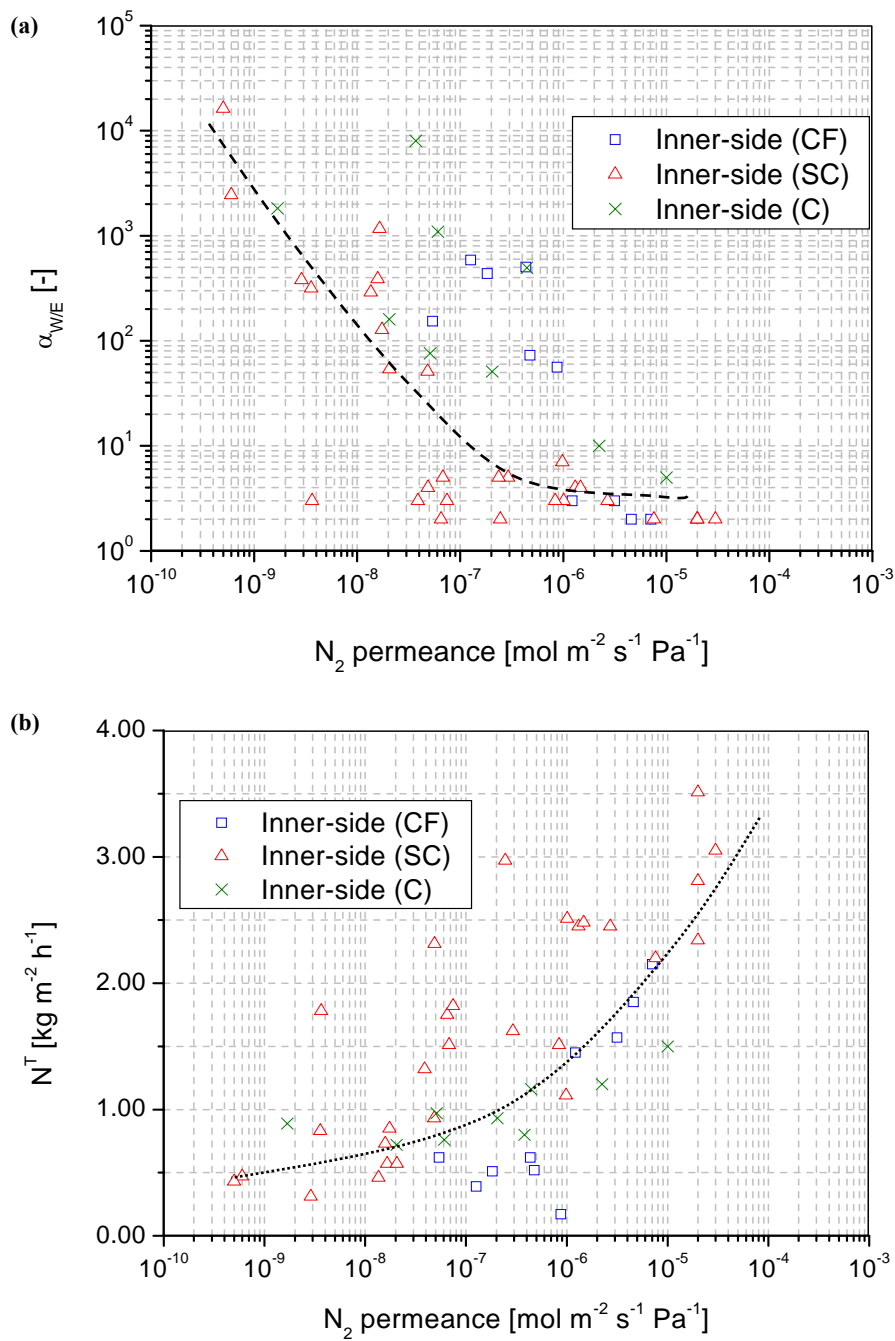


Figure IV.39 Evolution of (a) water/ethanol selectivity and (b) total flux with N_2 permeance in the PV experiments for the inner-side zeolite NaA membranes. Synthesis conditions in Table IV.3. PV conditions as in Table IV.7. Dashed and dotted lines refer to the trends observed, respectively, for selectivity and total flux.

The general trends shown in Figure IV.38 indicate that membranes with N_2 permeances up to $10^{-8} - 10^{-9} \text{ mol m}^{-2} \text{ s}^{-1} \text{ Pa}^{-1}$ are generally expected to possess zeolite layers of good quality (see for instance the results reported by *Pina et al., 2004* for the preparation of outer-side tubular zeolite NaA membranes), while permeances in the $10^{-5} - 10^{-6} \text{ mol m}^{-2} \text{ s}^{-1} \text{ Pa}^{-1}$ for zeolite membranes of the type prepared in this work are a sure indication of a significant presence of meso- and macroporous defects. The effect of intercrystalline porosity in the loss of separation ability of the synthesized membranes towards water separation is illustrated in Figure IV.40.

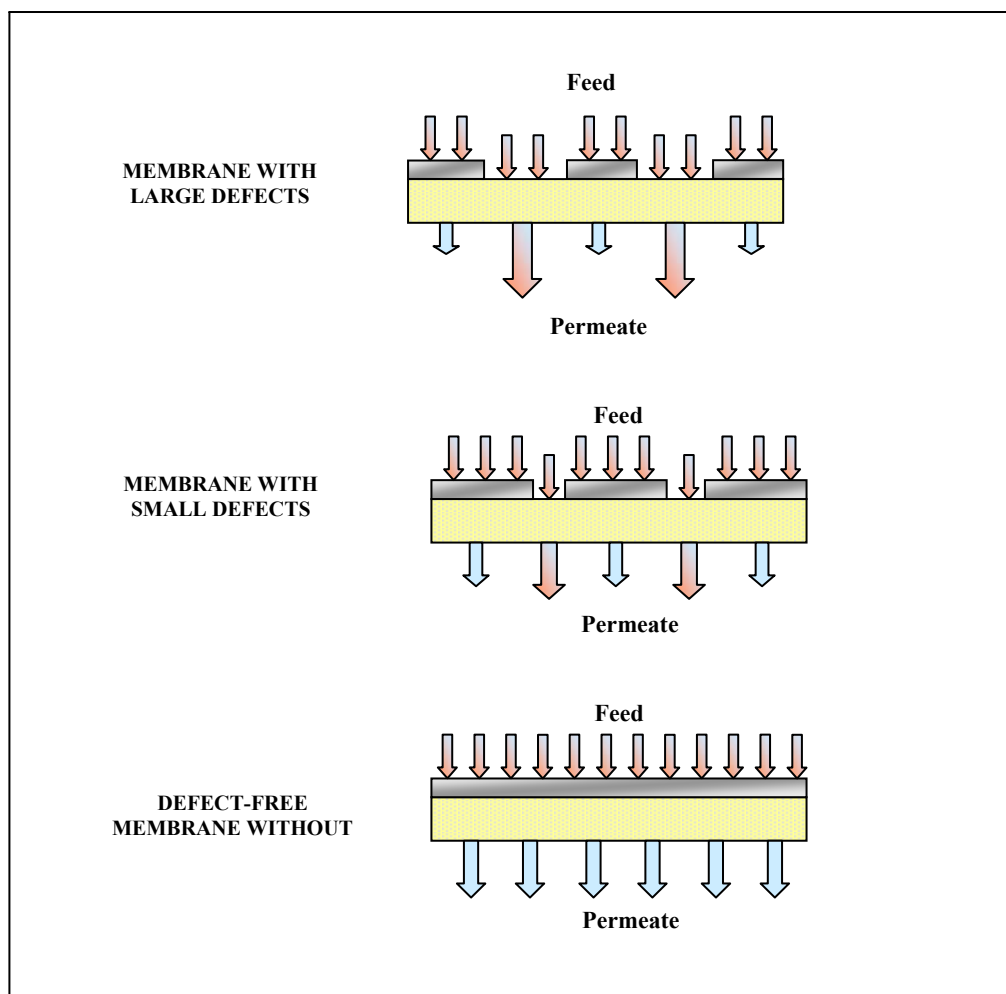


Figure IV.40: Morphologies of zeolite NaA layers and their influence in their pervaporation performance of water/ethanol liquid mixtures. Colors blue and red refer to water and ethanol, respectively.

Figure IV.41 shows the effect of the He/N₂ ideal selectivity in both the water/ethanol selectivity and the total flux of the inner-side zeolite NaA membranes synthesized under a centrifugal field listed in Table IV.7 for different SWG values and synthesis gels. As can be seen, the water/ethanol selectivity tends to increase with the He/N₂ selectivity, while the total flux does the opposite, in agreement with their general trends found with the N₂ permeance plotted in Figure IV.39. As the He/N₂ selectivity approaches the ideal Knudsen value (2.64), the membranes tend to show higher water/ethanol selectivities due to an increase in the continuity of the zeolite NaA layers and a reduction of the number of large defects.

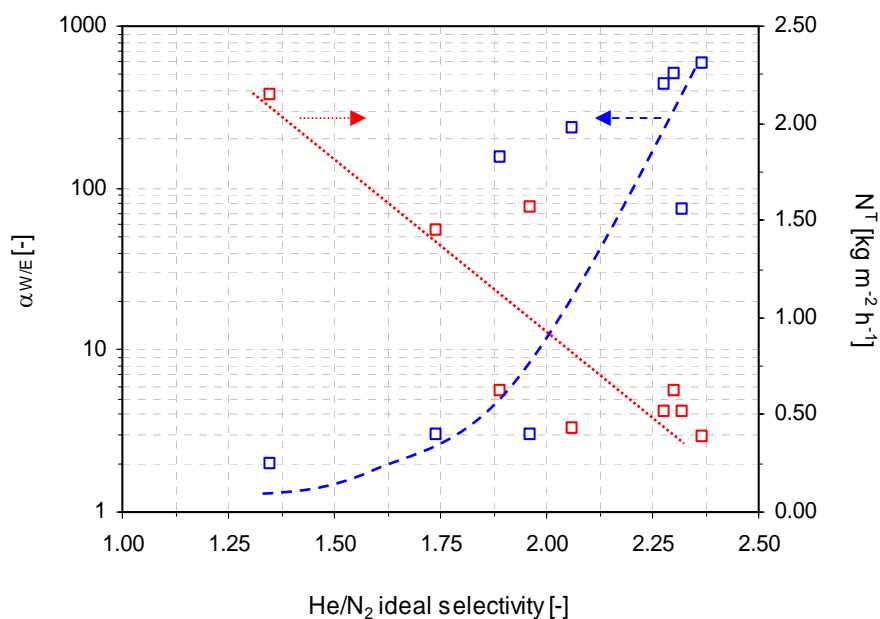


Figure IV.41: Evolution of water/ethanol selectivity and total flux with He/N₂ ideal selectivity in the PV experiments for the inner-side membranes prepared under a centrifugal field. Synthesis conditions: SWG= 0.05-1.75 mg cm⁻², 1-4 synthesis cycles, T=373 K, synthesis time=3 h, gels 1-3. PV conditions as in Table IV.7. Dashed and dotted lines refer to the trends observed, respectively, for selectivity and total flux.

It should be stressed that good quality membranes in terms of their PV performance towards the separation of water/ethanol mixtures have been prepared with He/N₂ ideal selectivity values never overcoming the ideal Knudsen value. These results suggest that the adsorption and diffusion of water across the zeolite crystals is dominant, although some non-zeolitic meso- and macroporosity still exists in the layers. Evidence of the presence of large defects in the *as*-synthesized membranes could be inferred by SF₆ single gas permeance experiments in the inner-side membranes prepared in the semi-continuous method. Ideal

N_2/SF_6 selectivities up to 2.10 were obtained, which are lower than the ideal Knudsen selectivity value (2.28), which reflects that a number of large pores with a mean pore size higher than the kinetic diameter of SF_6 , 0.55 nm, must be present in the zeolite layer. Despite this fact, on the grounds of strong hydrophilic adsorptive character of zeolite NaA crystals, mass transfer through zeolite pores is expected to be dominant and therefore the effect of the defects to the overall mass transfer might become partially compensated. As a result, the membranes would show the experimental observation that they are able to dehydrate organic mixtures.

IV.5.3. Effect of the weight gain after synthesis

The effect of the weight gain in the PV performance of the inner-side zeolite NaA membranes prepared under a centrifugal field and in the semi-continuous and continuous systems under widely different conditions (number of cycles, SWG, renewal rate, seeding method) is shown in Figure IV.42. Notwithstanding a considerable dispersion due to the different conditions used, it can be seen that, as could be expected, water/ethanol selectivities show a positive trend with the weight gain, while the total flux tends to decrease. From the results presented in Figure IV.42, it seems that a weight gain in the range 5-10 mg cm⁻² is needed to obtain good PV selectivity for membranes prepared under a centrifugal field (3-4 synthesis cycles) and for membranes prepared in a continuous system (1 synthesis cycle). However, a minimum weight gain around 15 mg cm⁻² is needed to obtain good PV selectivity for the membranes synthesized in the semi-continuous system.

When comparing these values with those reported on previous works (e.g., *Tiscareño-Lechuga et al., 2003; Pina et al., 2004*), it is interesting to note that the loading of zeolite material for the preparation of inner-side membranes under a centrifugal field and in the continuous system that display good PV performance is similar to that found for outer-side membranes. However, for membranes prepared in the semi-continuous system, this value can be as much as twice to that for outer-side membranes. The presence of a great number of gel pulses at high renewal rates (1/7-1/4 min⁻¹) in the semi-continuous system seems to make more difficult to prevent the membranes prepared with this method from defect formation, requiring thicker layers for the same separation selectivity.

IV.5.4. Effect of the SWG

Figures IV.43 and IV.44 show the role of the SWG in the separation selectivity and total flux, respectively, of the inner-side zeolite NaA membranes synthesized under a

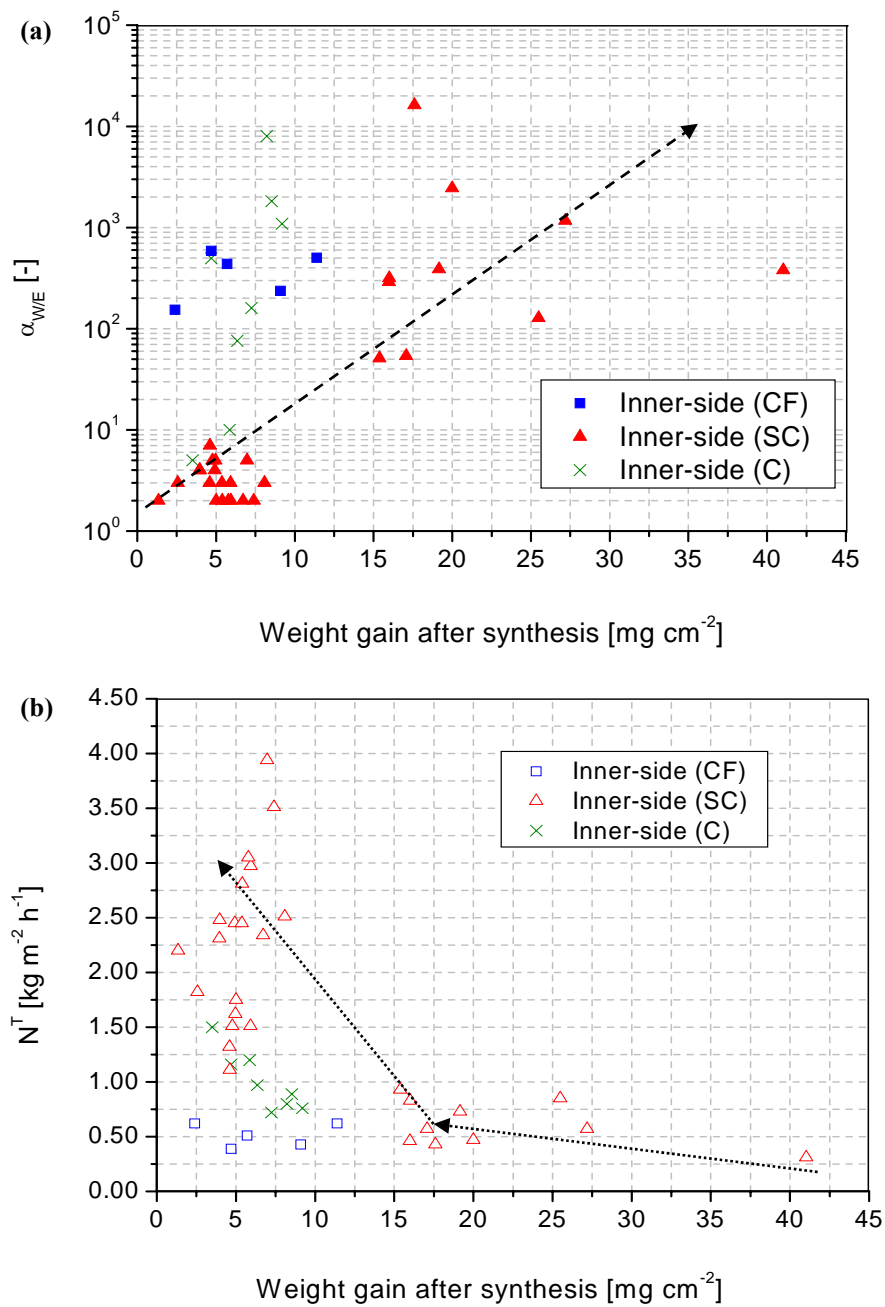


Figure IV.42: Evolution of (a) water/ethanol selectivity and (b) total flux with the weight gain after synthesis in the PV experiments for the inner-side membranes prepared in this work. Synthesis conditions as in Table IV.3. PV conditions as in Table IV.7. Dashed and dotted arrows refer to the trends observed, respectively, for selectivity and total flux.

centrifugal field and in the semi-continuous system (gel renewal rates in the range $1/16$ - $1/4$ min^{-1}) seeded by both the brush and cross-flow seeding techniques. The pattern observed resembles that already shown in Figures IV.23 and IV.24 for the effect of the SWG in the weight gain of the membranes after synthesis. As can be seen in Figures IV.43 and IV.44a, a maximum in the water/ethanol selectivity appears to be observed for SWG values, respectively, in the ranges 0.35-0.40 and 0.15-0.20 mg cm^{-2} , the latter range irrespective of the renewal rate used, although good selectivity values were only found for renewal rates of $1/7$ min^{-1} and higher. The explanation in this case could be the same for the results in Figures IV.23 and IV.24: higher values of the SWG lead to unstable seed layers from which lumps of seeds are easily detached, giving rise to seedless areas that, after synthesis result in discontinuities and membrane defects that lead to low pervaporation selectivity. For lower and higher SWG values, the membranes provide a poor ethanol/water selectivity, which is in agreement with the results already presented for N_2 permeances and He/N_2 selectivities.

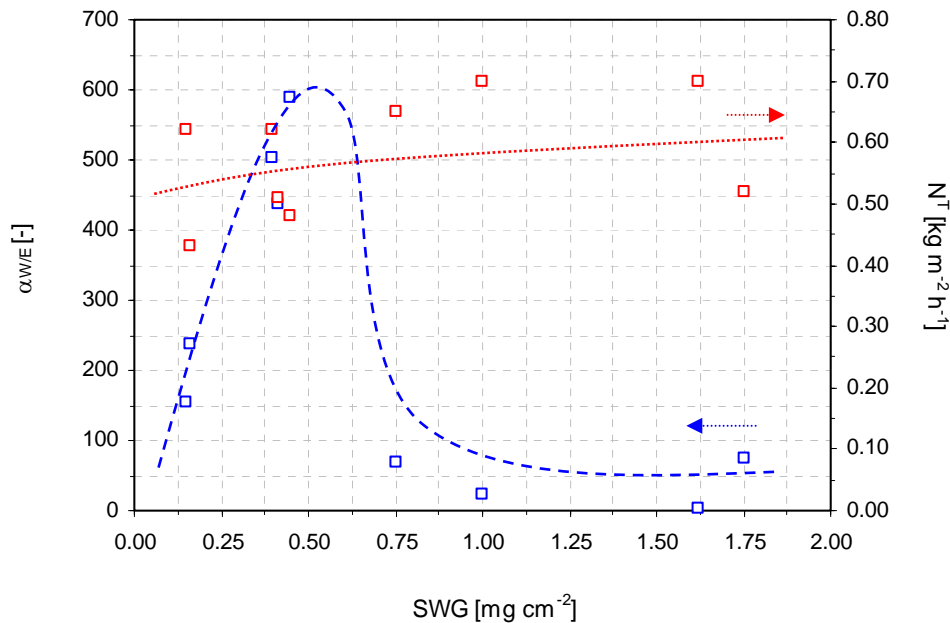


Figure IV.43: Evolution of water/ethanol selectivity and total flux with the SWG in the PV experiments for the inner-side membranes prepared under a centrifugal field. Synthesis conditions: SWG= 0.05-1.75 mg cm^{-2} , 1-4 synthesis cycles, $T=373$ K, synthesis time=3 h, gels 1-3. PV conditions as in Table IV.7. Dashed and dotted lines refer to the trends observed, respectively, for selectivity and total flux.

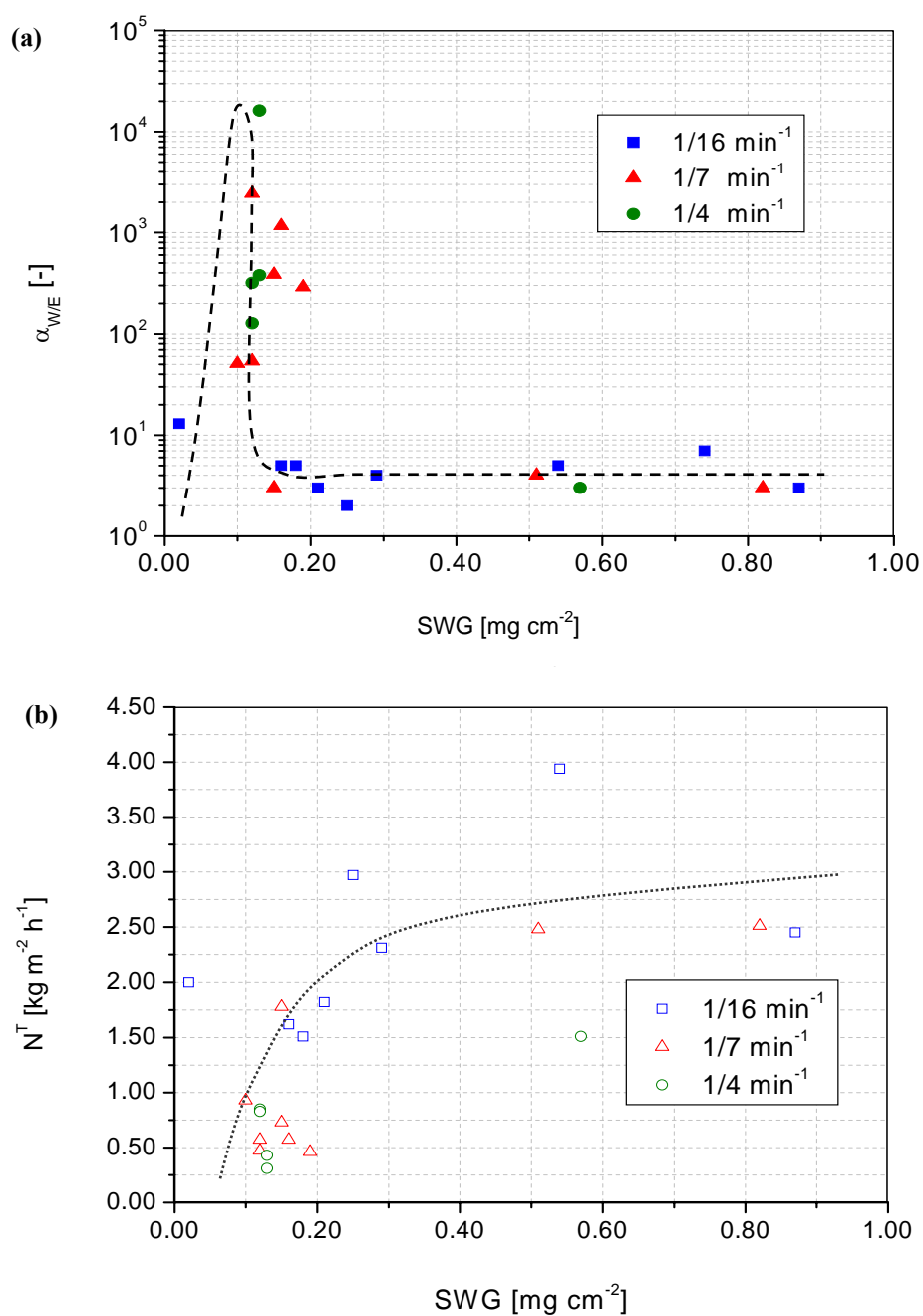


Figure IV.44: Effect of the SWG in (a) water/ethanol selectivity and (b) total flux in the pervaporation experiments for the inner-side zeolite NaA membranes membranes prepared in the semi-continuous system for gel renewal rates 1/16-1/4 min⁻¹. Synthesis conditions: SWG=0.15-0.87 mg cm⁻², arrangement III.8b in the autoclave, T=368 K, synthesis time=5 h, 1-2 cycles. PV conditions as in Table IV.7. Dashed and dotted lines refer to the trend observed, respectively, for selectivity and total flux.

Furthermore, the effect of the SWG in the total flux for the membranes synthesized in the semi-continuous system is shown in Figure IV.44b. As can be seen, despite the dispersion of the experimental results, a positive trend of the total flux with the SWG can be proposed in agreement with the trend observed for the total flux in Figure IV.43 for the membranes synthesized under a centrifugal field. It should be emphasized that the positive trend of the PV total flux with the SWG is in agreement with the positive trends found for the N₂ permeance and the weight gain after synthesis with the SWG depicted in Figures IV.23 and IV.24. The reason for such trend might be again ascribed to the impossibility to grow a continuous zeolite NaA layer when the SWG increases because of a higher number of meso- and macroporous defects.

IV.5.5. Effect of the number of synthesis cycles

Figure IV.45 shows the evolution of the water/ethanol selectivity and total flux with the number of synthesis cycles for the inner-side membrane ZA-INN-CF-02 prepared under a centrifugal field and membrane ZA-INN-SC-22 prepared in the semi-continuous system. As can be seen, the total flux tends to decrease with the number of synthesis cycles for both membranes. Furthermore, regarding the effect of the number of synthesis cycles in the water/ethanol selectivity, an increase with the number of synthesis cycle is observed, which becomes very sharp for membrane ZA-INN-CF-02 after the third synthesis cycle. The reduction of total flux and enhancement of the selectivity of the membranes with the number of synthesis cycles might be ascribed to an increase in the thickness of the zeolite layer formed and to a reduction in the number of large defects. However, it should be noted that the water/ethanol selectivity shows a decrease after the fourth synthesis cycle for membrane ZA-INN-CF-02, which could involve certain dilution of some zeolite material as was pointed out by Kumakiri *et al.* (2000).

Ideally, a zeolite membrane prepared in only one synthesis cycle with a good PV performance is desired. However, this is often far impossible to be achieved due to the presence of some defects or mesoporosity after one cycle. The experience gathered in this work reveals that the renewal of the gel in the lumen of the support is essential to reduce the number of cycles in the preparation of inner-side zeolite NaA membranes. In this way, as it is pointed out in Figure IV.45, the membranes prepared with gel renewal by the action of a centrifugal field usually require at least 3 synthesis cycles to achieve a good PV performance, while those prepared in the semi-continuous system usually require 1-2. Finally, the membranes synthesized in the continuous system showed the best PV performance in only 1 synthesis cycle due to higher gel renewal compared to that of the other synthesis methods.

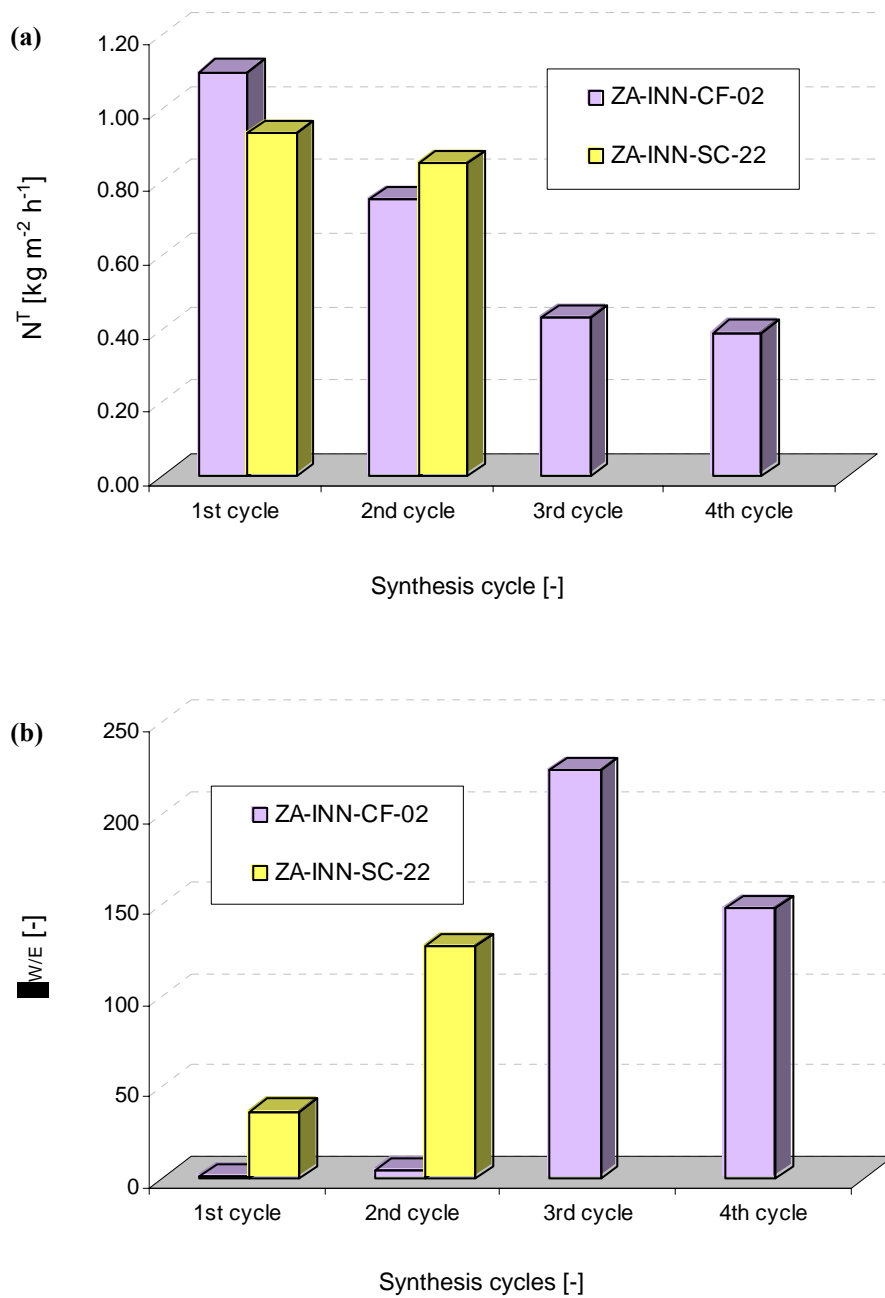


Figure IV.45: Evolution of (a) total flux and (b) water/ethanol selectivity with the number of synthesis cycles in the PV experiments for membrane ZA-INN-CF-02. Synthesis conditions: SWG=0.20 mg cm⁻², ω =100 r.p.m, T = 373 K, 3 synthesis cycles, gel 1. PV conditions as in Table IV.7.

IV.5.6. Stability of the membranes

The stability of two of the inner-side membranes prepared in this work under a centrifugal field (ZA-INN-CF-03) and in the continuous system (ZA-INN-C-06) were tested towards the VPV of a 92 : 8 ethanol/water liquid mixture at 323 K. (see Figure IV.46). As can be seen, both membranes preserved their separation effectiveness during at least 230 h, with a water/ethanol selectivity around 220 and a flux around $0.40 \text{ kg m}^{-2} \text{ h}^{-1}$ for membrane ZA-INN-CF-04 and 8000 and $0.80 \text{ kg m}^{-2} \text{ h}^{-1}$, respectively, for membrane ZA-INN-C-06.

It should be stressed that the membranes synthesized in this work usually preserve their PV performance when stored in a liquid environment. However, the membranes tend to suffer from thermal stress when they are subjected to a number of operation and drying cycles, which tend to damage their structure and generate a number of cracks that remove their separation ability.

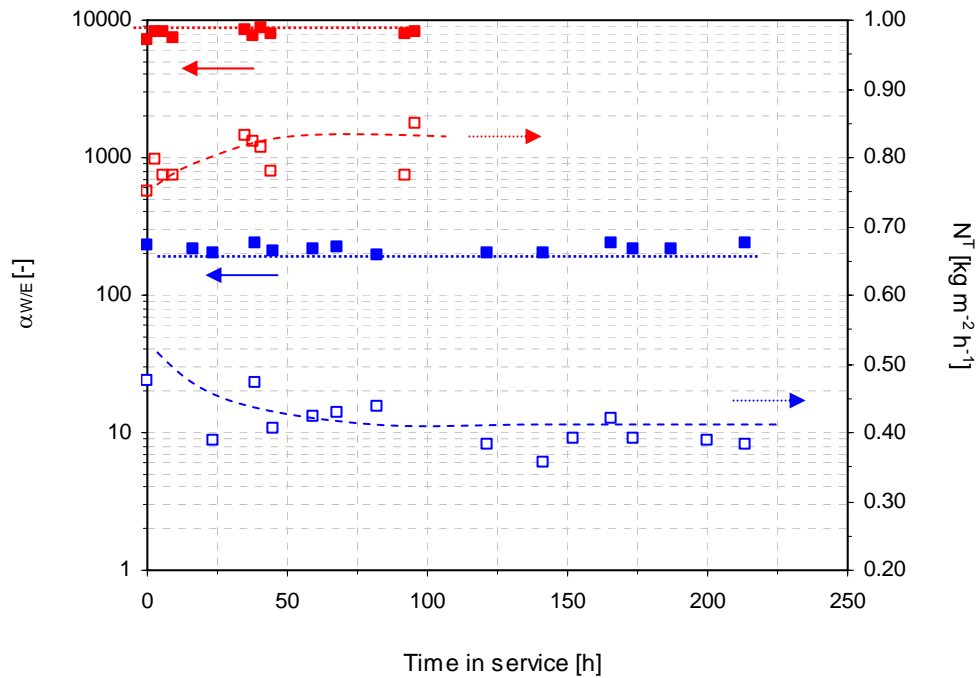


Figure IV.46: Water/ethanol selectivity and total flux as a function of time. Blue and red symbols refer, respectively, to membranes ZA-INN-CF-03 (SWG=0.45 mg cm^{-2} , $\omega=100$ r.p.m, 3 synthesis cycles, gel 2) and ZA-INN-C-02 (SWG=0.13 mg cm^{-2} , 1 synthesis cycle, gel flow rate= 1.5 mL min^{-1} , T=353 K, synthesis time=6 h, gel 4). PV conditions as in Table IV.7. Dashed and dotted lines refer to the trends observed, respectively, for selectivity and total flux.

IV.6. DISCUSSION AND FINAL REMARKS

In view of the results obtained and discussed in the previous sections, both outer- and inner-side tubular zeolite NaA membranes prepared with the outlined methods and in the optimal conditions appear to be promising for the dehydration of ethanol/water mixtures by PV. Table IV.8 summarizes the experimental seeding and synthesis conditions for the zeolite NaA membranes synthesized in this work that showed the highest reproducibility, as well as water/ethanol selectivities and total fluxes that can be attained.

In light of the results exposed in Table IV.8, the inner-side membranes prepared in the continuous system onto TiO₂ supports with a previous brush-seeding step show the best PV performance, because this technique allows a continuous gel renewal in the lumen of the tubular supports. It should be highlighted that, compared to the other synthesis methods, in addition to the higher water/ethanol selectivities, the total flux across the *as*-synthesized membranes is nearly twice the value of that of the membranes prepared under a centrifugal field. This value is higher than that reported by *Kondo et al. (1997)* and approaches the results reported by *Van den Berg et al. (2003)* (see Table V.9). Furthermore, these membranes allow good PV performance with 9-10 mg cm⁻² zeolite material, the half of the weight required for the semi-continuous system to achieve good PV performance, which is crystallized onto the support in only 1 synthesis cycle.

The membranes with the best PV performance allow the dehydration of ethanol/water mixtures with low feed water content (~5-8 wt.%), and with water composition in the permeate up to 99% at the tested conditions. The selectivities reported in this work for inner-side tubular zeolite NaA membranes approach the high values reported for outer-side and flat membranes. The outstanding dehydration ability shown by these membranes allow them to be promising candidates for dehydrating organic mixtures by PV as an alternative to distillation. Moreover, because the flux across these membranes is high compared to that of polymeric and other inorganic membranes, zeolite NaA membranes appear to be also promising in terms of membrane area requirement.

Table IV.8: Optimal conditions for the preparation of outer- and inner-side tubular zeolite NaA membranes. PV conditions as in Table IV.7.

Membrane configuration	Reactor Configuration ¹	Seeding and synthesis conditions			Primary characterization		PV performance ^{3,4}		
		Seeding Technique ²	SWG [mg cm ⁻²]	T [K]	Time [h] / Cycles	Weight gain [mg cm ⁻²]	N ₂ permeance [mol m ⁻² s ⁻¹ Pa ⁻¹]	Q _{w/E} [-]	N ^F [kg m ⁻² h ⁻¹]
Outer-side	Semi-continuous (AC) (1/38-1/13 min ⁻¹)	Rubbing	0.48-0.73	373	5 / 1	6-9	10 ⁻⁸ – 10 ⁹	325 ± 92	3.53 ± 0.54
Inner-side	Centrifugal field (VS) (100 r.p.m)	C-F filtration	0.20-0.40	373	3 / 3-4	5-10	10 ⁻⁷ – 10 ⁸	325 ± 64	0.51 ± 0.05
	Semi-continuous (AC) (1/7-1/4 min ⁻¹)	C-F filtration Brush-seeding	0.15-0.20	363-373	5 / 2	15-20	10 ⁻⁸ – 10 ⁹	830 ± 350	0.56 ± 0.08
	Continuous (AC) (1.5-4 mL min ⁻¹)	Brush-seeding	0.12-0.20	353-363	6-7 / 1	5-10	10 ⁻⁸ – 10 ⁹	2831 ± 1738	0.91 ± 0.09

¹ Notation: AC (Autoclave); VS (Vessel open to the atmosphere)² C-F filtration: Cross-flow filtration³ Confidence interval 95%⁴ The temperature was 373-379 K for outer-side membranes and 323 K for inner-side membranes

Table IV.9: PV performance of zeolite NaA membranes towards the dehydration of EtOH/water liquid mixtures

Thickness [μm]	Support	X_w [wt.%]	T [K]	$\alpha_{w/E}$ [-]	N^f [$\text{kg m}^{-2} \text{h}^{-1}$]	Reference
7	TiO ₂ (rutile) inner tube	10	323	2800	0.91	Pera-Titus et al. (2006b) (This study)
15-20	α -Al ₂ O ₃ inner tube	8	323	830	0.56	Pera-Titus et al. (2006a) (This study)
30	α -Al ₂ O ₃ inner tube	8	323	325	0.51	Pera-Titus et al. (2005) (This study)
NA	mullite tube	5	298	>10000	0.68	Kazemimoghadam et al. (2004)
		10	298	884	0.46	
10	α -Al ₂ O ₃ outer tube	10	398	3600	3.80	Pina et al. (2004)
7	α -Al ₂ O ₃ inner tube	9	366	130	2.5	Tiscareño-Lechuga et al. (2003)
3.5	TiO ₂ disk	5	318	54000	0.86	Van den Berg et al. (2003b)
NA	ZrO ₂ / C Sheet	5	298	2000	0.065	Jafar et al. (2002)
		10	298	1500	0.079	
		10	323	1000	0.16	
		10	343	900	0.18	
30	α -Al ₂ O ₃ outer tube	5	348	16000	1.10	Okamoto et al. (2001)
		10	348	10000	2.16	
		10	323	1700	0.79	

Table IV.9 (to be continued)

Thickness [μm]	Support	X_w [wt, %]	T [K]	$\alpha_{w/E}$ [-]	N^T [$\text{kg m}^{-2} \text{h}^{-1}$]	Reference
7	$\alpha\text{-Al}_2\text{O}_3$ disk	10	298	3000	0.072	Braunbarth et al. (2000)
5	SS outer tube	5	313	150	0.050	Holmes et al. (2000)
		10	313	180	0.079	
30	Mullite outer tube	10	333	1000	1.20	Shah et al. (2000)
4	$\alpha\text{-Al}_2\text{O}_3$ disk	10	303	10000	1.00	Kumakiri et al. (1999)
10	mullite outer tube	5	323	4800	0.40	Kondo et al. (1997)
		10	323	46000	0.77	
		10	348	42000	2.16	
		10	393	47000	8.47	